

PROJECT ADMINISTRATION DATA SHEET

ORIGINAL REVISION NO. _____

Project No. E-25-A05 (R6059-OA6) GTRC/XXX DATE 10 / 24 / 85

Project Director: S. M. Jeter/W. J. Wepfer School/XXX Mechanical Engr.

Sponsor: Georgia Power Company

Type Agreement: Letter of Acceptance Task RP1 under BOA 95

Award Period: From 9/18/85 To 12/31/85 (Performance) 6-30-86 (Reports) 12/31/85

Sponsor Amount: This Change 7/30/87 Total to Date

Estimated: \$ 34,628 \$ 34,628

Funded: \$ 34,628 \$ 34,628

Cost Sharing Amount: \$ None Cost Sharing No: N/A

Title: Analysis and Simulation of Variable Speed Drive Heat Pumps

ADMINISTRATIVE DATA

OCA Contact R. Dennis Farmer X4820

1) Sponsor Technical Contact: Gary L. Birdwell 2) Sponsor Admin/Contractual Matters: Same as 1)

Georgia Power Company

333 Piedmont Avenue, NE (20th Floor)

Atlanta, GA 30308

526-7359

Defense Priority Rating: N/A Military Security Classification: N/A

(or) Company/Industrial Proprietary: See Below

RESTRICTIONS

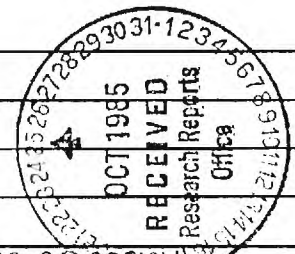
See Attached N/A Supplemental Information Sheet for Additional Requirements.

Travel: Foreign travel must have prior approval - Contact OCA in each case. Domestic travel requires sponsor approval where total will exceed greater of \$500 or 125% of approved proposal budget category.

Equipment: Title vests with Sponsor

COMMENTS:

A Non-Disclosure Agreement has been Negotiated.



COPIES TO: SPONSOR'S I. D. NO. 02.256.000.86.0051817

Project Director Procurement/GTRI Supply Services GTRC
Research Administrative Network Research Security Services Library
Research Property Management Reports Coordinator (OCA) Project File
Accounting Research Communications (2) Other A. Jones

2-N
SR-130

GEORGIA INSTITUTE OF TECHNOLOGY
OFFICE OF CONTRACT ADMINISTRATION

NOTICE OF PROJECT CLOSEOUT

Date 7/13/89

Project No. E-25-A05

Center No. R6059-0A6

Project Director Dr. S. M. Jeter; Dr. W. J. Wepfer

School/Lab ME

Sponsor Georgia Power Company

Contract/Grant No. BOA95 - Task RPI

GTRC XX GIT

Prime Contract No. N/A

Title Analysis and Simulation of Variable Speed Drive Heat Pumps

Effective Completion Date 7/30/87 (Performance) 7/30/87 (Reports)

Closeout Actions Required:

- None
- Final Invoice or Copy of Last Invoice
- Final Report of Inventions and/or Subcontracts
- Government Property Inventory & Related Certificate
- Classified Material Certificate
- Release and Assignment
- Other _____



Includes Subproject No(s). _____

Subproject Under Main Project No. _____

Continues Project No. _____ Continued by Project No. _____

Distribution:

- Project Director
- Administrative Network
- Accounting
- Procurement/GTRI Supply Services
- Research Property Management
- Research Security Services

- Reports Coordinator (OCA)
- GTRC
- Project File
- Contract Support Division (OCA)
- Other _____

PROGRESS REPORT TO
GEORGIA POWER COMPANY
ANALYSIS & SIMULATION OF
VARIABLE SPEED DRIVE HEAT PUMPS
S. M. JETER & W. J. WEPFER PIs
G. FADEL, N. COWDEN, A. DYMEK

GEORGE W. WOODRUFF
SCHOOL OF MECHANICAL ENGINEERING
GEORGIA INSTITUTE OF TECHNOLOGY
ATLANTA, GA 30332-0405
DECEMBER 11, 1985

PROJECT PROGRESS REPORT

1. Introduction

The simulation system under development will realistically model the simple vapor-compression heat pump system illustrated in Figure 1. Modular programming techniques and generic component modules are used throughout; consequently, the analytical techniques and software tools developed in this project can be applied to similar, but more complex, cycles as used or proposed in HVAC applications or in industrial processing.

Presently, four component modules have been completed for modeling the system. The interaction between the modules is expressed in the information flow diagram shown in Figure 2. The system shown in Figure 2 operates at constant speed. A motor module is under development and will be added to simulate variable speed operation.

The structure of the simulation program can be explained with reference to Figure 3. As shown in this flow-chart, cycle analysis begins with a guess of all the module outputs. Most importantly this guess includes values for the condenser pressure, P_c , and evaporator pressure, P_e .

The inner recycle loop includes the "high pressure side" components: compressor, condenser, and expansion valve. Using the guessed value of P_e , this loop is iterated until a convergent value for P_c is obtained. The detailed steps are:

- (a) Call compressor model to compute mass flow from guess of P_c .

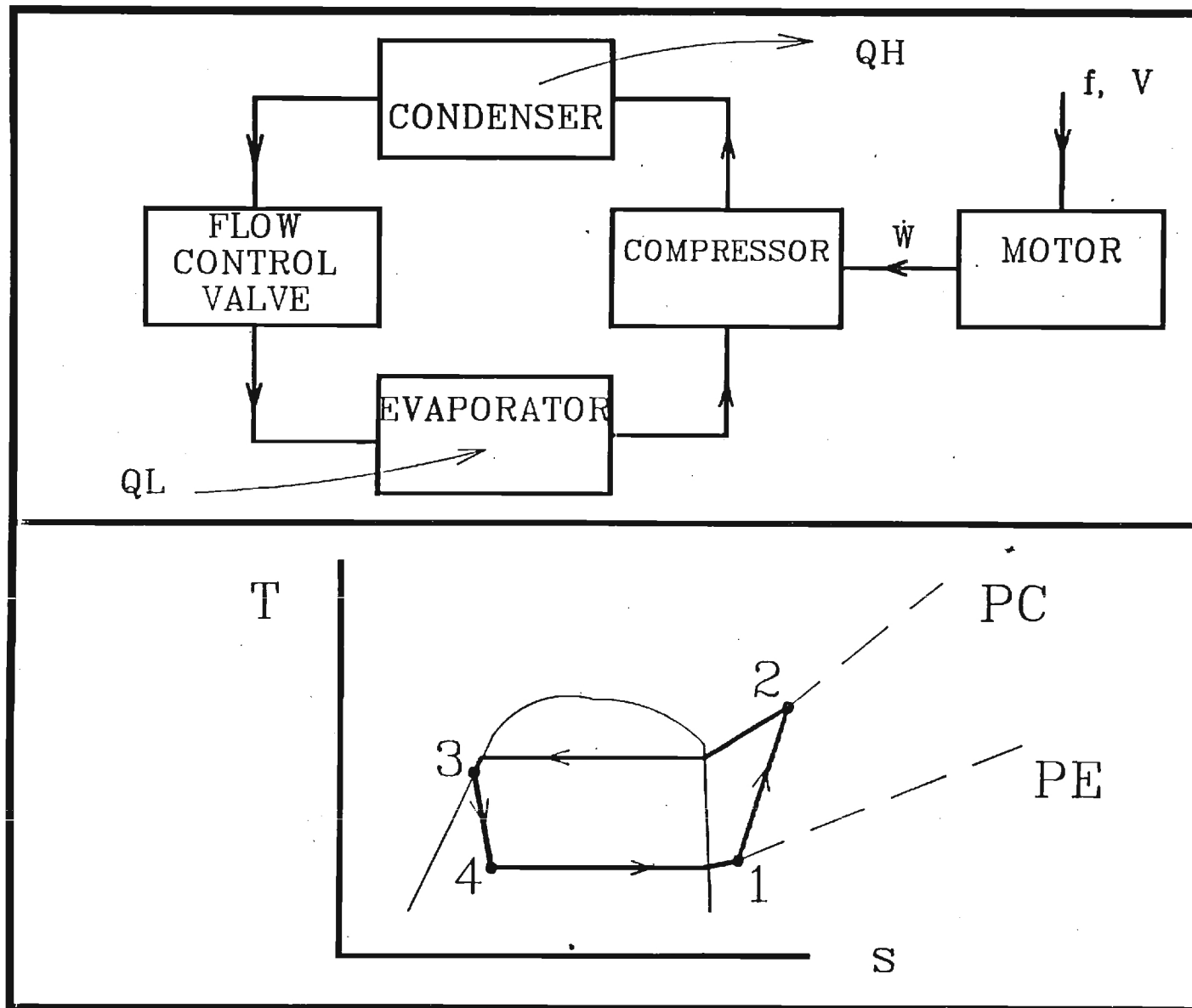


Figure 1. Simple Vapor-Compression Heat Pump System

INFORMATION FLOW DIAGRAM

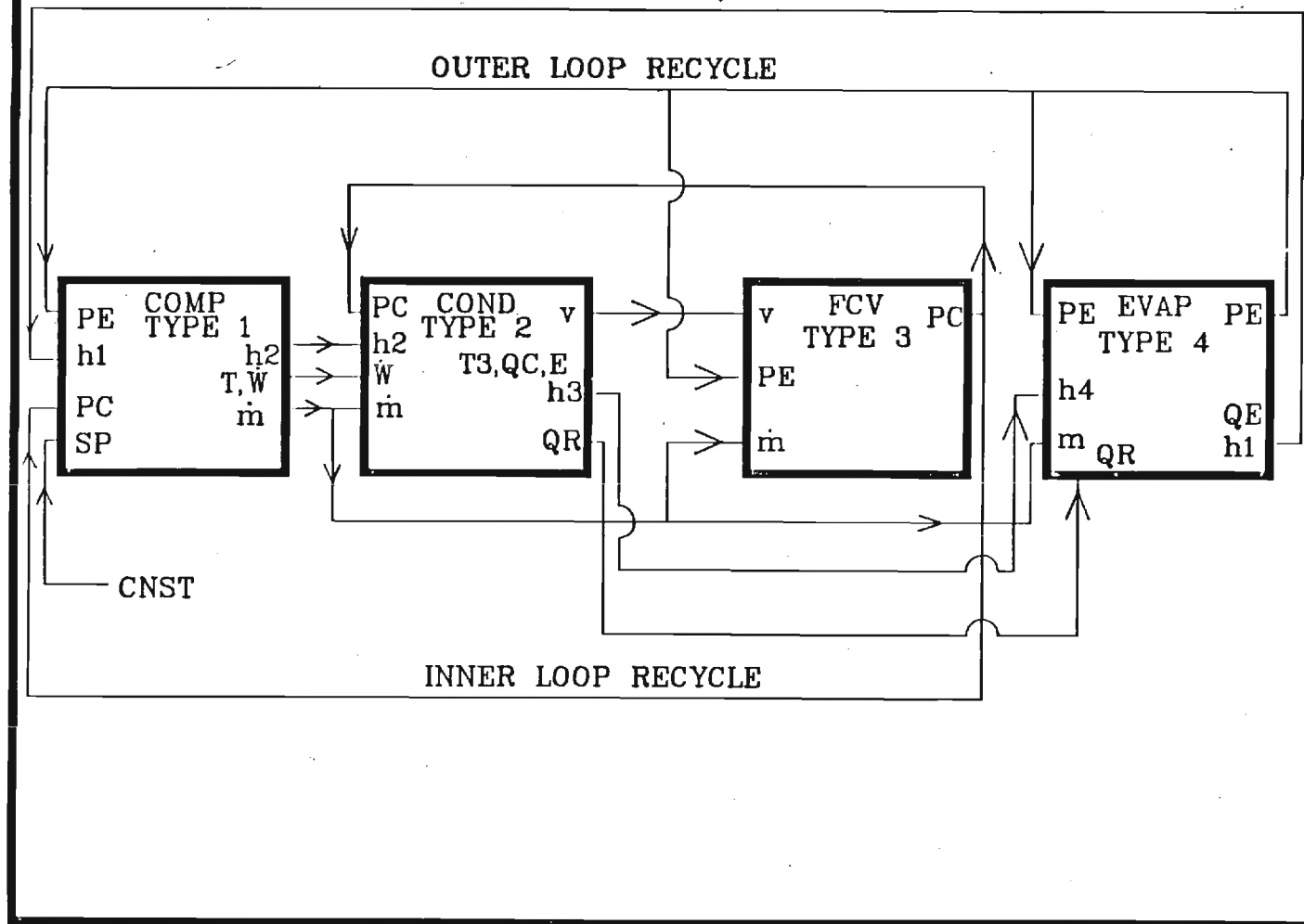


Figure 2. Information Flow Diagram for Constant Speed Operation.

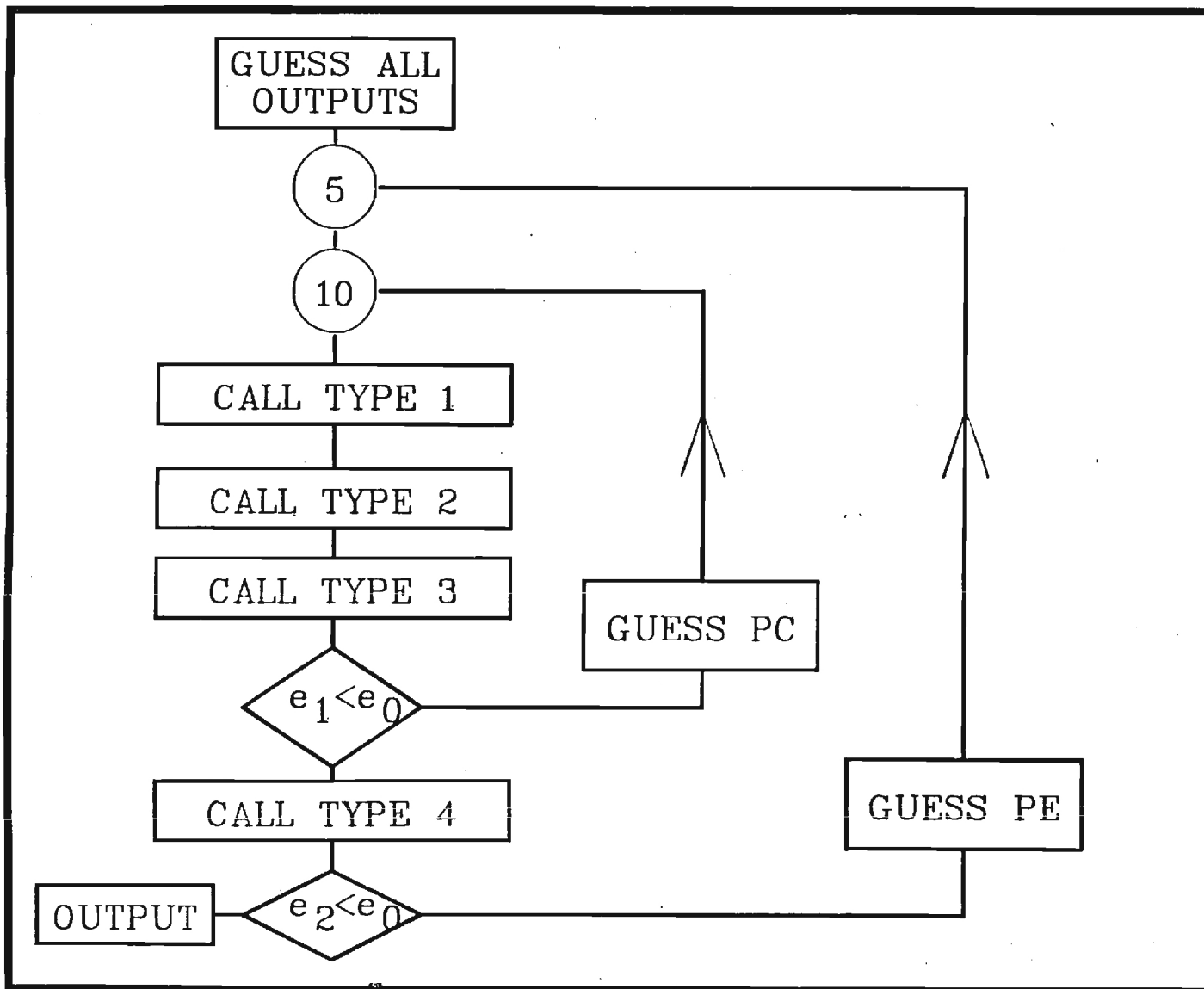


Figure 3. Program Flow Chart.

- (b) Call condenser model to compute heat rate and state of exit fluid.
- (c) Call valve model to compute P_c based on P_e , mass flow, and state of fluid from condenser.

Note that any vapor in the condenser exhaust would result in a large value for P_c . Consequently, these components realistically model the actual cycle performance which insures a slightly subcooled condensate.

The outer recycle loop is entered when a satisfactory P_c has been obtained. The evaporator (low-side heat exchanger) module is called. It computes the evaporator heat transfer rate as well as an estimate of the evaporator pressure, P_e , required for use in the overall steady-state energy balance:

$$Q_e = Q_c - W$$

Q_e = evaporator heat rate

Q_c = condenser heat rate

W = compressor power

Numerical simulation of this cycle is rather challenging because of the sensitivity of the operating state to the condenser and evaporator pressures. Reasonably efficient operation has been attained using Wegstein's method shown in Figure 4. As applied to the inner loop, assume P_1 is the first guess of the condenser pressure. Assume this guess is high, the compressor flow will be small and the condenser temperature and effectiveness high insuring a subcooled condensate. The valve module will thus compute a low pressure, CP_1 , to force a liquid

SOLUTION PROCEDURE

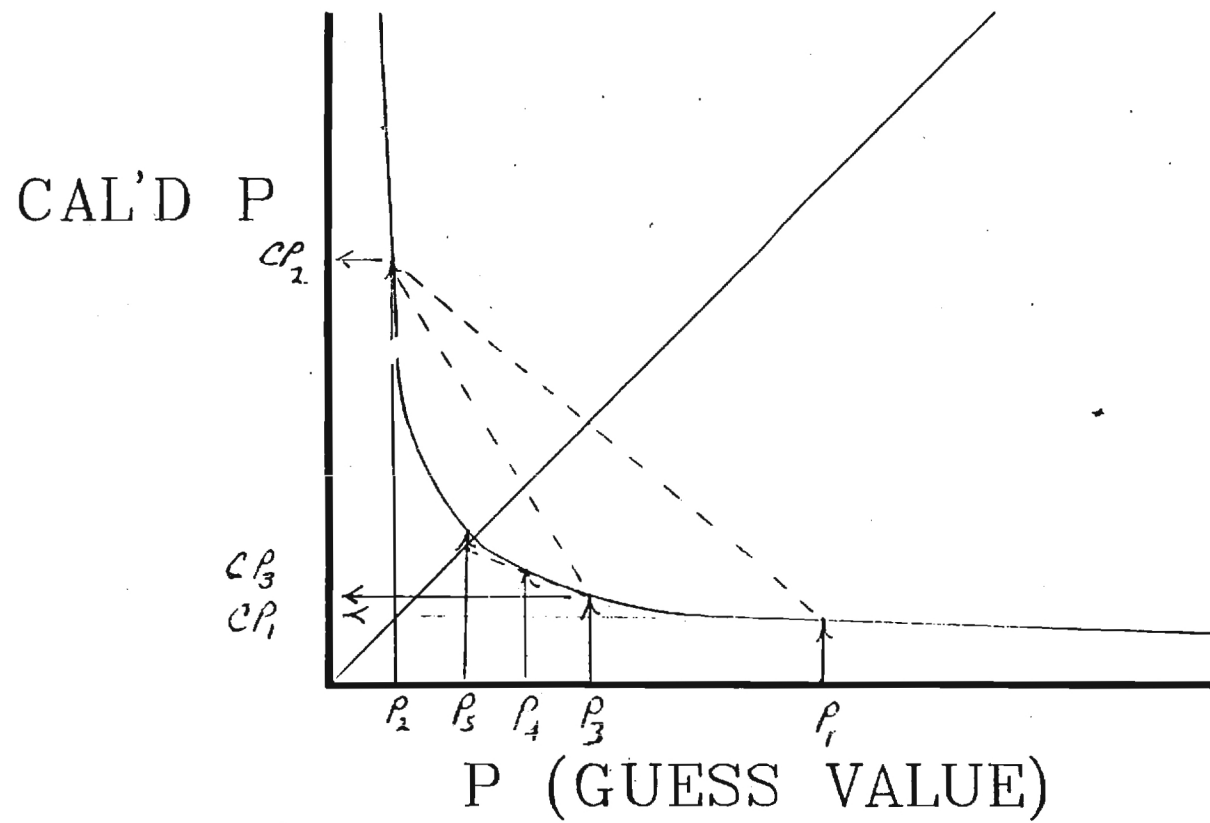


Figure 4. Graphical Representation of Weinstein's Procedure.

through the restriction at a low rate. This calculated value is taken as the next guess, P_2 . Assume it is now somewhat low. The compressor flow increases and the condenser temperature and effectiveness also decrease making it likely that some of vapor will be in the condenser exhaust. This vapor will greatly increase the volumetric flow and pressure drop in the valve resulting in a large calculated, CP_2 .

Continued resubstitution would result in oscillation between the extreme pressures. Instead the last two calculated pressure values are interpolated to the main diagonal, resulting in a guess of P_3 . This process is continued with guesses of P_4 , P_5 , etc. until convergence is obtained. This technique appears very promising for efficient simulation of the system.

2. Heat Exchangers

Two heat exchanger modules have been developed: the high-side (high pressure) and the low-side (low pressure) heat exchangers. The high side heat exchanger (Figure 5) requires as input the refrigerant properties and flow rate leaving the compressor. In addition, all tube, configuration, and geometric information as well as the inlet air state appear as parametric inputs. The heat transfer coefficients for the desuperheat, condensing and subcooled sections are computed in the high side heat exchanger module. The module first computes the desuperheat section heat transfer and area and then proceeds to the condensing section. Upon computation of the condensing section heat transfer, a test is performed to determine the exit state of the refrigerant and if any subcooling occurs. If subcooling does occur, the module computes

HIGH-SIDE HEAT EXCHANGER

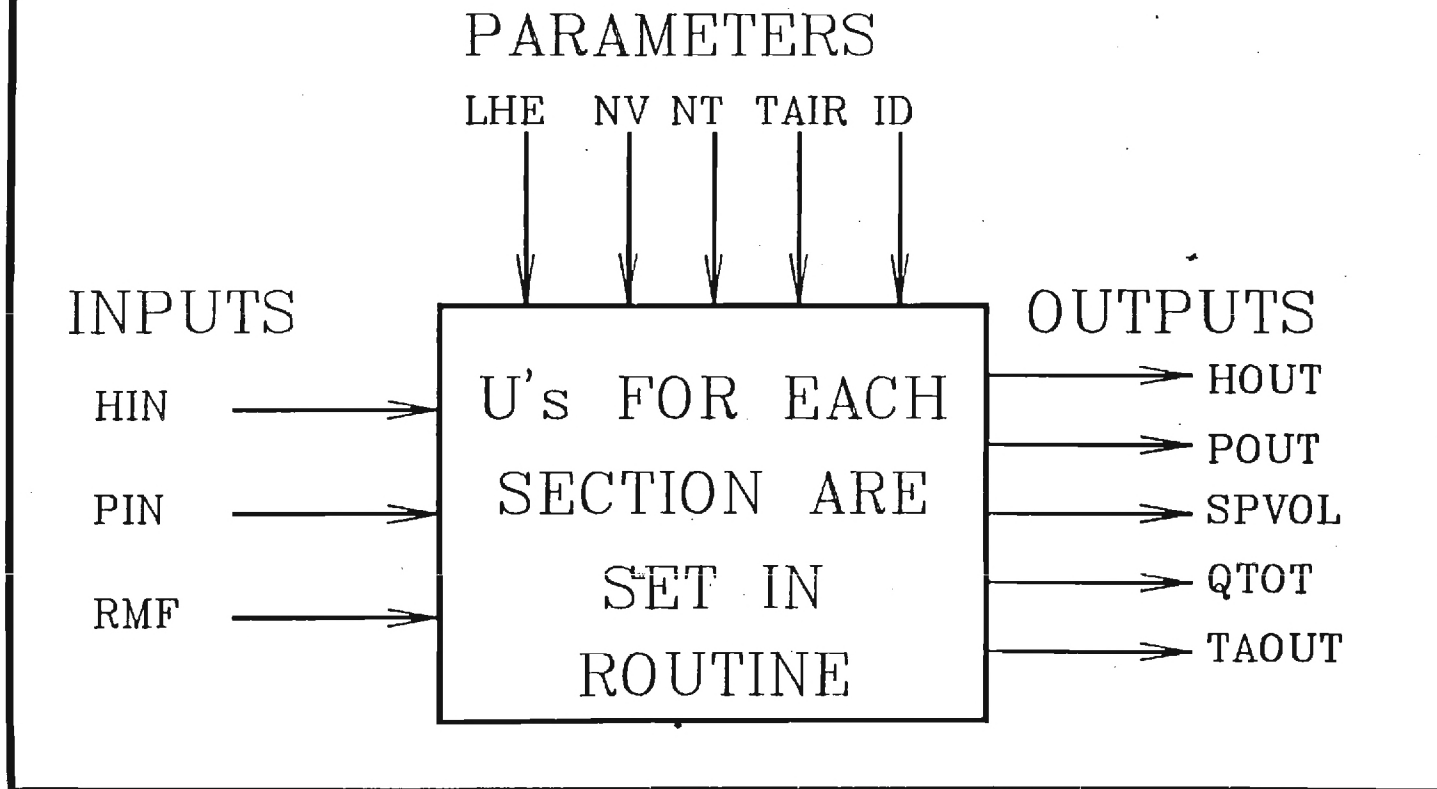


Figure 5. High-Side Heat Exchanger.

the subcooling area, heat transfer rate, and refrigerant exit state. The module also computes the total high-side heat transfer as well as the exit air state.

The low-side heat exchanger (Figure 6) requires the following variables as inputs: indoor air temperature, refrigerant flow rate and inlet enthalpy, "guessed" low-side pressure, compressor power, and the high-side heat transfer. Parametric inputs include: heat exchanger area, volumetric flow rate of indoor (or return) air, air pressure and heat capacity, and an iteration error tolerance. The module calculates the number of heat exchanger transfer units, the effectiveness, and the low-side heat transfer rate. The module then updates the low-side temperature (and hence the low-side pressure) based on a comparison with the high-side heat transfer rate and the compressor power:

$$Q_{LR} \text{ (required low-side heat transfer)} = Q_H - W$$

$$Q_L \text{ (calculated low-side heat transfer)}$$

$$T_E = T_A - [Q_{LR}/Q_L][T_A - T_{EOLD}]$$

$$T_A = \text{inlet air temperature}$$

$$T_E = \text{updated low-side temperature}$$

The module recomputes the NTU, effectiveness, and low-side heat transfer until the required and calculated low-side heat transfer rates converge to within the user specified error tolerance. The module outputs the exit refrigerant state (including the updated low-side pressure), the low-side heat transfer, and the exit air state.

3. Fan Submodules

The fan submodule (Figure 7) requires as input variables the speed

LOW-SIDE HEAT EXCHANGER

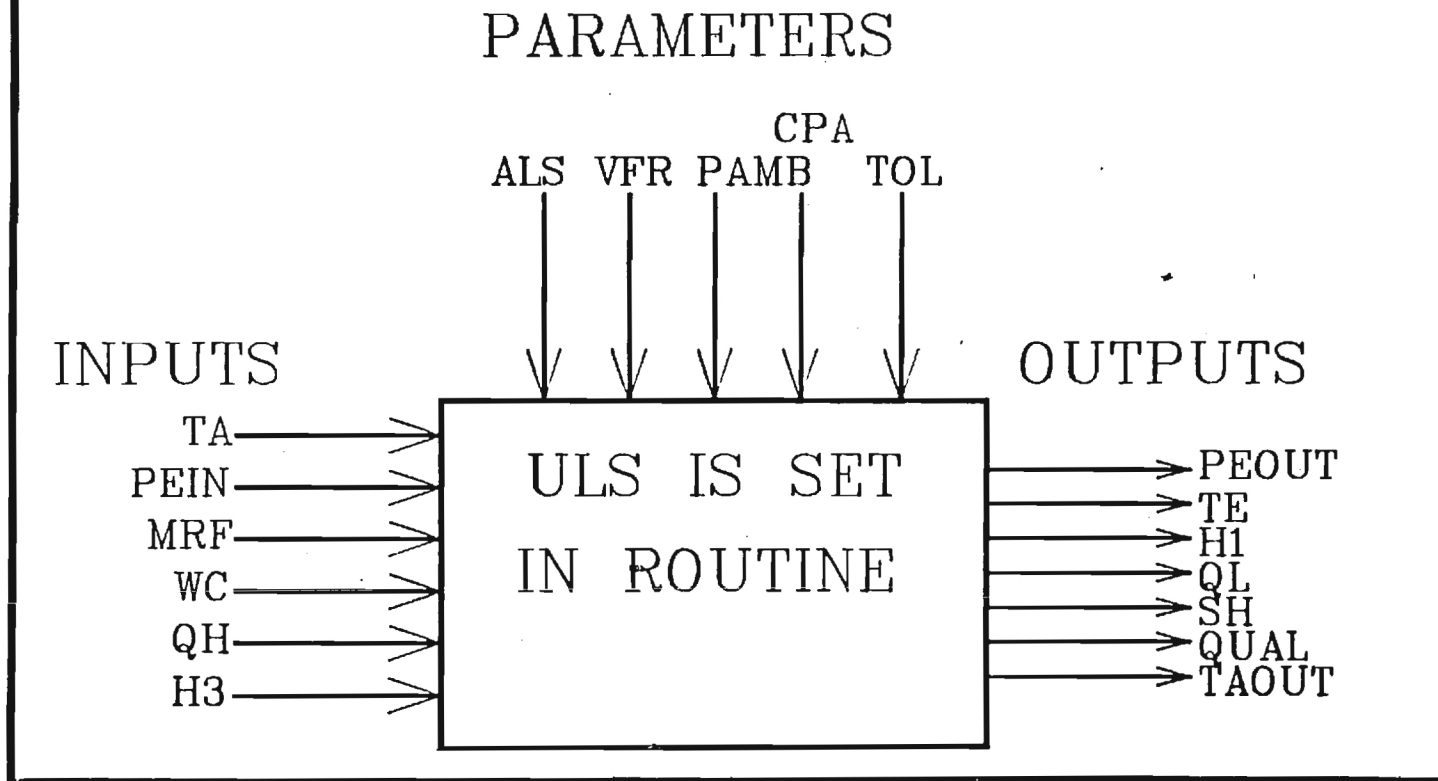


Figure 6. Low-Side Heat Exchanger.

FAN SUBMODULE

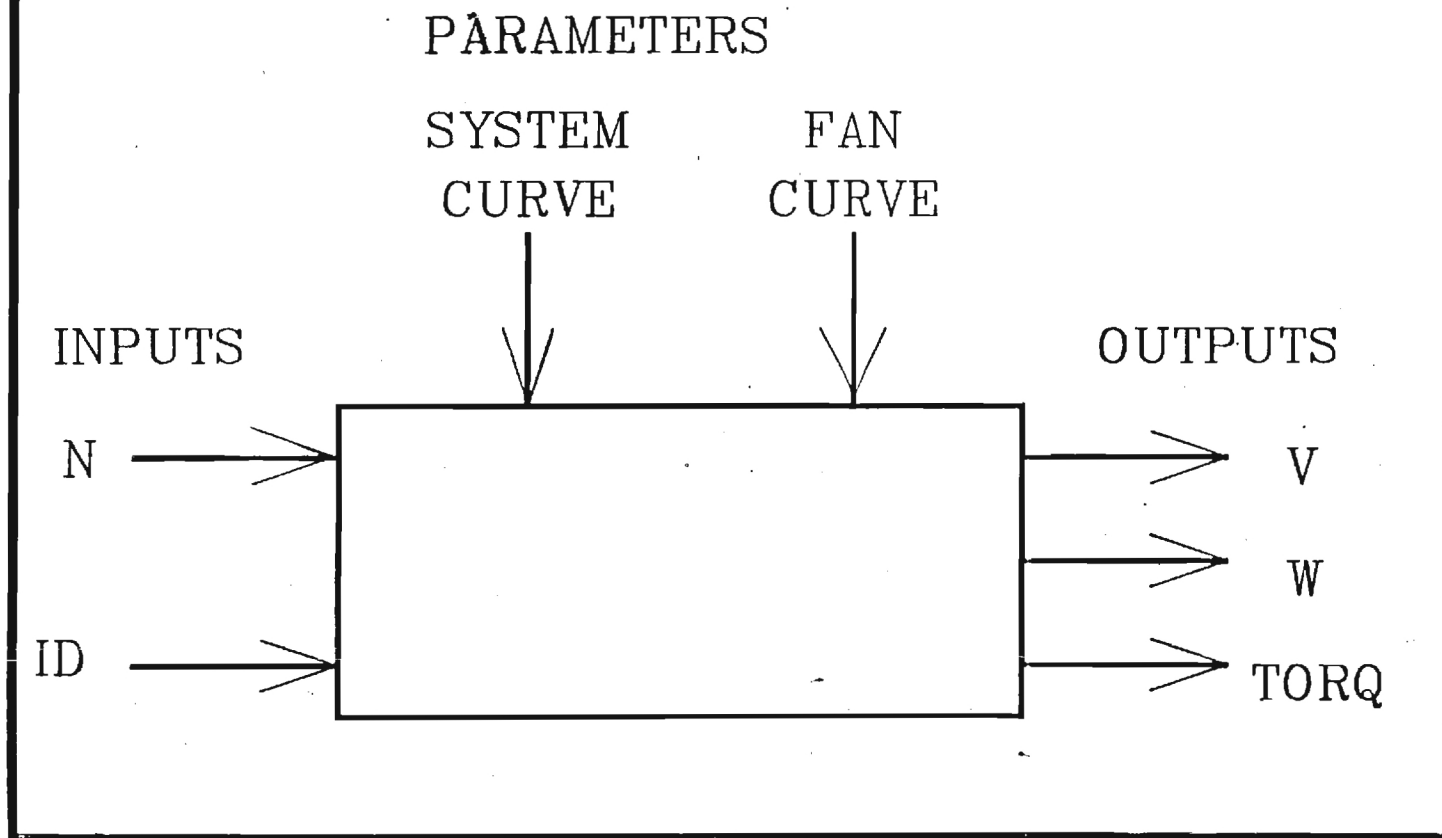


Figure 7. Fan Submodule.

and an indicator variable(ID). The indicator variable is set from the executive routine and tells the module whether the fan is an axial outdoor fan or a centrifugal indoor fan. The fan and system curves are input as parametric information. The algorithm adjusts the fan curves for the specified RPM using the well-known fan laws, and solves the non-linear fan and system curves for the operating point. The module outputs the fan torque and power as well as the volumetric flow rate. The fan submodules are currently being integrated into the heat exchanger modules.

4. Compressor

The compressor (Figure 8) is a realistic model which should be reliable and flexible. A reciprocating compressor is assumed. The thermodynamic cycle is as follows:

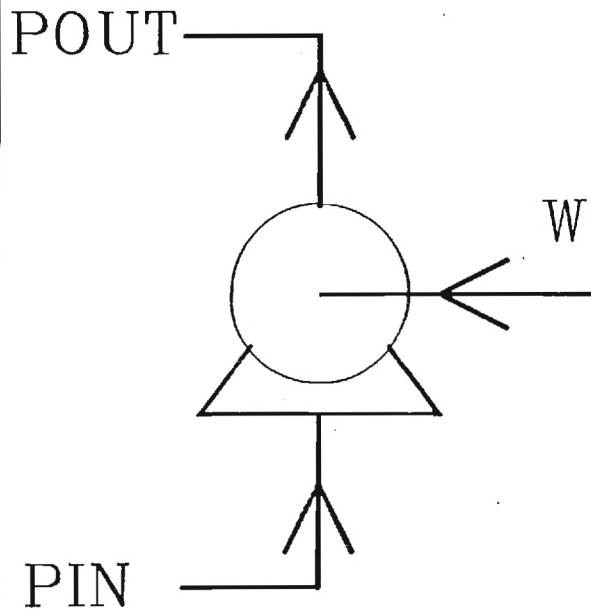
- (a) An inlet valve pressure drop is modeled using a valve flow coefficient, C_v :

$$P = k[V/C_v]^2$$

- (b) A constant-pressure inlet stroke is assumed.
- (c) Irreversible compression is modeled using a polytropic process.
- (d) An exhaust valve pressure drop is modeled again using a C_v model.
- (e) Irreversible expansion is modeled using a polytropic process.

The module computes the exhaust state, flow rates, and for interaction with the motor modules, the average torque. The several parameters can be adjusted to simulate actual compressors. Possible

COMPRESSOR



1. SIMPLE BUT REALISTIC
2. INCLUDES:
INLET VALVE ΔP
CONST P INTAKE
IRREVERSIBLE
COMPRESSION
EXIT VALVE ΔP
IRREVERSIBLE
EXPANSION
3. OUTPUTS:
FLOW, TORQUE
& EXIT STATE

Figure 8. Compressor Module.

enhancements include a speed-dependent mechanical friction component.

5. Flow Control Valve

The flow control valve (Figure 9) is modeled using a valve flow coefficient:

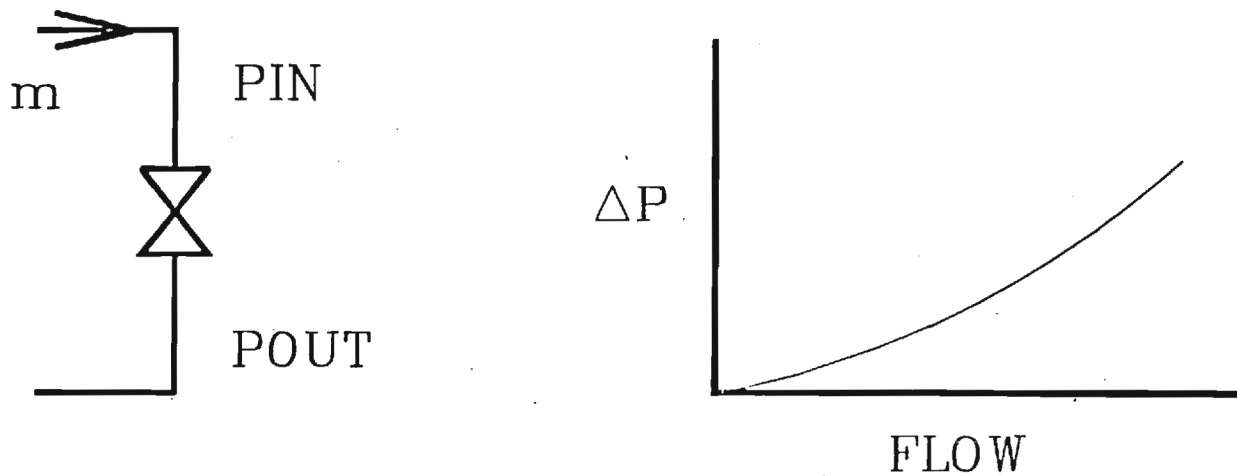
$$P_{IN} = P_{OUT} + [V/C_v]^2$$

The coefficient and possibly the exponent can be adjusted to model physical components.

Various control schemes can be modeled. Presently a fixed C_v , such as a conventional capillary tube, is modeled. Feedback can be included to model controlled expansion valves such as the common devices that respond to evaporator superheat. Response to condensate subcooling is also possible.

Intelligent control of the expansion valve could enhance cycle efficiency by allowing minimum condenser pressure and maximum evaporator pressure. Such intelligent control can also be modeled.

FLOW CONTROL VALVE



1. SIMPLE VALVE COEFFICIENT MODEL

$$\Delta P = [\dot{V}/C_v]^2$$

2. CAN INCLUDE VARIOUS CONTROL SCHEMES

- A. FIXED C_v , CAPILLARY
- B. EVAPORATOR SUPERHEAT
- C. CONDENSER SUBCOOLING
- D. INTELLIGENT CONTROL

Figure 9. Flow Control Valve.

WINTER QUARTER PLANS

1. The first part of the Winter Quarter work involves the refinement and validation of the modules:

FAN/COILS: Include dehumidification effects, improved heat transfer and friction factor coefficients (using the Reynolds Analogy), improved fan and system curves.

COMPRESSOR: Include a speed-dependent mechanical friction term, parameter identification including exit/inlet valve coefficients, and polytropic expansion and compression coefficients.

FLOW CONTROL: Include feedback and investigate other control schemes (modes).

MOTORS: Variable frequency and voltage control.

2. Investigate and implement the system control scheme. Perhaps a simple PI or even a PID controller is best (Figure 10). Work will focus on the interaction of the heat pump, house, thermostat, and inverter.

3. Annual Bin Calculations

A simple method for comparing the annual performance of the variable speed heat pump (VSHP) and constant speed heat pump (CSHP) uses hourly temperature bins. Various references indicate the number of hours per year the ambient conditions are contained in temperature intervals or bins (e.g. 95 F to 99 F).

Assuming the heat pumps are properly suited to their loads, at extreme conditions they run continually to meet the maximum load:

$$Q_m = UA[T_r - T_{a,e}] = Q_{HP}(T_r, T_{a,e})$$

HEAT PUMP SYSTEM CONTROL

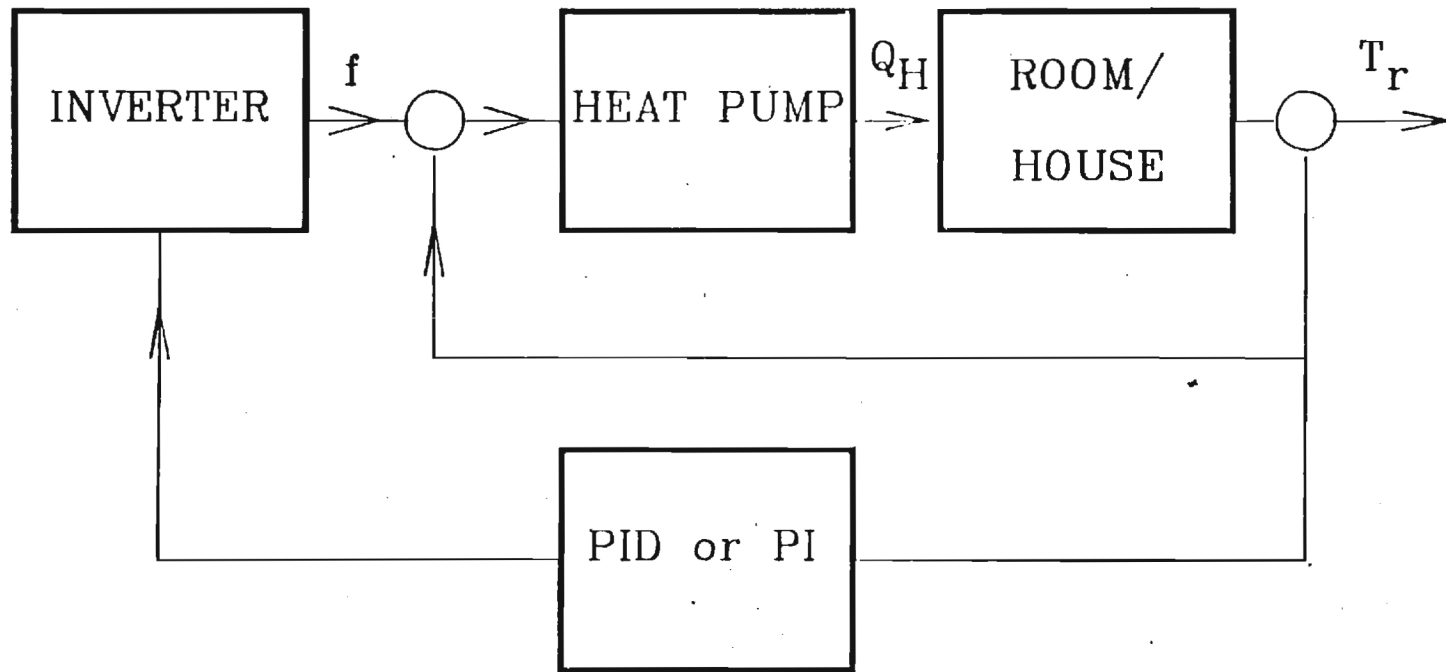


Figure 10. System Control Block Diagram.

Q_m = maximum heating load

UA = building UA

T_r = room temperature

$T_{a,e}$ = extreme ambient temperature

Q_{HP} = heat pump heat rate for specified conditions

The previous calculation gives the proper building UA. For less extreme conditions, the CSHP will cycle (run part of the hour). For a given bin then:

$$Q_B = UA(T_r - T_{a,e})[1 \text{ hour}] = Q_{CS}\Delta t$$

where:

Q_{CS} = heat rate of the CSHP

$\Delta t < 1$ hour

The CSHP will consume electric energy for this bin in the amount:

$$W_{CS} = Q_B / \text{COP}_{CS}$$

The VSHP will run the entire hour but at a lower speed and a higher COP to meet the load:

$$Q_B = Q_{VS}[1 \text{ hour}]$$

and will consume a smaller amount of electrical power given by:

$$W_{VS} = Q_B / \text{COP}_{VS}$$

This calculation will provide an early indication of the relative merit of the two designs.

SPRING/SUMMER QUARTER PLANS

Spring and Summer Quarter activities will focus on full season simulations (and appropriate validation) to include integration of the house modules, variable speed controllers, and the full heat pump model.

GEORGIA POWER COMPANY GENERAL PURCHASING AGREEMENT

ADVANCED TECHNOLOGY TASK STATEMENT BOA-95

PROJECT NAME: ANALYSIS & SIMULATION OF VARIABLE SPEED DRIVE HEAT PUMPS

PRINCIPLE INVESTIGATORS: S. M. Jeter & W. J. Wepfer
George W. Woodruff School of Mechanical Engineering

PURPOSE: To improve and enhance a modular computer simulation program for studying the performance of heat pumps with variable speed drive in comparison with conventional heat pumps and heat pumps with superheat recovery.

SCOPE AND PROCEDURE:

1. Improve fan/heat exchanger modules to include improved heat transfer analysis, to model variable fan speeds, and to include dehumidification.
2. Improve compressor model to interact with variable speed motors, to include mechanical friction, and to include better component parameter estimates.
3. Include various expansion valve control schemes.
4. Conduct annual temperature - bin performance analysis.

PERSONNEL AND BUDGET (WINTER QUARTER, 1986):

<u>% Time</u>	<u>Salary/Amount</u>	<u>Fringe (21%)</u>	<u>Overhead (63.5%)</u>	<u>Total</u>
Sheldon M. Jeter (25%)	3,087	648	2,372	6,107
William J. Wepfer (25%)	3,392	712	2,606	6,710
Research Engineer (33%)	2,340	491	1,798	4,629
GRA (33%)	2,000		1,270	3,270
GRA (33%)	2,000		1,270	3,270
Travel	500		318	818
Materials & Supplies	500		318	818
TOTALS:	\$12,819(Salary) \$ 1,000(Misc)	\$1,851	\$9,952	\$25,622
Less Georgia Tech Sponsored GRA	(\$2,000)		(\$1,270)	(\$3,270)
Less Carry Over from Fall 1985				(\$10,800)
Amount Requested, Winter Quarter 1986				(\$11,552)

FALL QUARTER 1985 BUDGET STATUS

	<u>BUDGETED</u>	<u>EXPENDED</u>
PIs	\$8551.35	\$8551.35
GRA ¹	4000.00	2121.99
G. FADEL	2340.00	454.00
G. FADEL (PROJECTED)	-----	1000.00
TRAVEL	1000.00	500.00
COMPUTER TIME	2000.00	-----
MATERIALS & SUPPLIES	1000.00	150.00
FRINGE (21% OF PI)	2287.00	1795.78
OVERHEAD (63.5%)	13449.00	9254.25
TOTAL	<u>\$34627.35</u>	<u>\$23827.37</u>

¹N. E. COWDEN IS SUPPORTED VIA A "STELSON" GRA

DELIVERABLE ITEM: Improved heat pump models and preliminary results comparing the performance of variable speed with conventional drive.

INTERIM REPORT

ANALYSIS AND SIMULATION OF VARIABLE SPEED DRIVE HEAT PUMPS

Sheldon M. Jeter, Associate Professor
William J. Wepfer, Associate Professor
Georges M. Fadel, Graduate Research Assistant
Norman E. Cowden, Graduate Research Assistant
Andrew A. Dymek, Graduate Research Assistant

The George W. Woodruff
School of Mechanical Engineering
GEORGIA INSTITUTE OF TECHNOLOGY
Atlanta, GA 30332-0405

INTERIM REPORT

Prepared for

GEORGIA POWER COMPANY

Report Period Covering:
January 1, 1986 to June 30, 1986

June 10, 1986

TABLE OF CONTENTS

I. INTRODUCTION AND STATUS.....1

II. DESCRIPTION OF MODULES.....2

 1. COMPRESSOR.....2

 1.1 ISENTROPIC COMPRESSOR MODEL.....2

 1.2 POLYTROPIC COMPRESSOR MODEL.....3

 2. FLOW CONTROL VALVE.....10

 3. SIMPLE HEAT EXCHANGER MODELS.....11

 4. DETAILED HEAT EXCHANGER MODELS.....14

 4.1 CONDENSER.....14

 4.2 EVAPORATOR.....15

 4.3 DESCRIPTION OF DESUP, CONDENS, SUBCOOL.....16

 4.4 CALCULATION OF VARIABLE FILM COEFFICIENTS.....17

 4.5 MODELING OF FAN PERFORMANCE.....18

III. DESCRIPTION OF SIMULATION SYSTEM.....19

 1. OVERVIEW.....19

 2. CONVERGENCE ROUTINES.....20

 3. UTILITY ROUTINES.....23

IV. ANNUAL BIN CALCULATIONS.....24

 1. DESCRIPTION.....24

 2. RESULTS.....27

V. FUTURE WORK.....29

VI. REFERENCES.....30

I. INTRODUCTION AND STATUS

This report summarizes work done under Georgia Power Company's Technology Development Center Task Statement BOA 95 Task RP1 on the Analysis and Simulation of Variable Speed Drive Heat Pumps for the period covering 1 January 1986 through 30 June 1986. We are pleased to report that the initial goals and objectives of this research program have been met. A modular simulation program for studying the performance of variable speed drive heat pumps relative to conventional constant speed heat pumps has been developed and successfully implemented. A simple variable speed heat pump is modeled using a polytropic compressor module, a constant coefficient flow control valve, and simplified heat exchanger modules. Seasonal performance is computed via a temperature bin analysis. Results indicate that the variable speed unit requires on the order of 6 to 10% less electrical energy than a comparable constant speed unit operating in the heating mode. These results do not penalize the conventional unit for cycling losses which can be significant.

Work has been completed on several component modules including a detailed compressor model, heat exchanger modules that account for variable film coefficients and variable fan coil speed, and a modified flow control valve. These modules will be tested with the existing simulation code and then used to obtain more accurate estimates of the energy and cost advantages of the electrically-driven variable speed heat pump.

II. DESCRIPTION OF MODULES

1. Compressor Modules

The compressor module was designed to simulate the operation of a variable-speed positive-displacement compressor. The module inputs include the exit state of the evaporator, the condenser pressure, and the frequency of the electrical power supplied to the compressor motor. Several other pertinent parameters are also required. Using this data, the module calculates the mass flow rate of the refrigerant, the electrical power required to compress the refrigerant, and the state at the outlet of the compressor.

During the course of this project two different modules were written. Both of the modules were developed assuming the compressor to be adiabatic. The first is a simple model that bases its calculations on the isentropic efficiency equation. This simple module was used as a prototype for the later more complicated module. The later module uses the concept of polytropic compression to calculate the needed quantities. It is more detailed in that it takes into account:

1. Heating of the refrigerant as it passes over the electric motor (assuming a hermetic compressor).
2. Pressure drops in the inlet and outlet valves.
3. Mechanical efficiency of the compressor.
4. Electrical efficiency of the motor.
5. Calculation of volumetric efficiency based on the clearance volume.

1.1 Isentropic Compressor Model. The simple module uses the isentropic efficiency equation to calculate the required quantities. The module starts by finding the hypothetical outlet state of the compressor based on an isentropic compression. The state is determined by calling the property routines [1] with the entropy of the inlet state and the pressure of the outlet state. The isentropic work per unit mass is then calculated from the difference between the inlet enthalpy and the exit isentropic enthalpy. With this, the actual work per unit mass can be found using the isentropic efficiency which is given as a parameter. The actual work is calculated by:

$$WA = WS/EFF$$

where WA and WS are the actual and isentropic work per unit mass and EFF is the isentropic efficiency. The actual exit enthalpy is found by adding the actual work to the inlet enthalpy. With the exit enthalpy and the condenser pressure (compressor exit pressure) the property routines are used to find the outlet state.

The compressor speed must be known in order to calculate the rate dependent quantities such as power and refrigerant flow rate. A

dimensionless torque vs. speed curve is used to characterize typical AC induction motor performance. The torque is nondimensionalized by dividing the torque by the locked rotor torque which is supplied as a parameter. This parameter can be changed to simulate different motors.

Since the torque, TRK, is just the work per radian, it can be calculated by:

$$TRK = (FPR*WA)/2\pi$$

where WA is the work per unit mass which is multiplied by the flow per revolution, FPR, to get work per revolution and divided by 2π to convert it to work per radian. FPR is found by:

$$FPR = (ETAV*DIS)/VIN$$

where ETAV is the volumetric efficiency, DIS is the compressor displacement (both are parameters), and VIN is the inlet specific volume. The TRK is then divided by the locked rotor torque to give the dimensionless torque that is used as the input to a table lookup routine which returns a dimensionless speed. The dimensionless speed is the speed divided by the synchronous speed of the compressor. For the typical two pole compressor motor construction, the synchronous speed equals the electrical frequency. Thus the compressor speed is found by multiplying the dimensionless speed by the frequency. Notice that by using this dimensionless speed the motor can be run at different frequencies.

Once the compressor speed is calculated, the refrigerant flow rate, FRM, follows as:

$$FRM = FPR*SP$$

where FPR is defined above and SP is the compressor speed. With the flow rate calculated, the compressor power, WDOT, can be found from:

$$WDOT = FRM*WA$$

where FRM and WA are defined above.

1.2 Polytropic Compressor Model. The more detailed compressor module better represents the actual process within an adiabatic hermetic compressor. This module accounts for the heat that is generated by the inefficiencies of the electric motor. This energy is absorbed by the refrigerant as it passes over the motor. The module also includes the pressure drop in the inlet and outlet valves. The compression and expansion processes are modeled using a polytropic relation to better simulate the actual process within the compression chamber.

Using a guess of the rotational speed, the module first calculates the work and, from that, the torque required to compress the refrigerant. Using the supplied motor torque speed curve (as in the simple module) the routine calculates the speed of the compressor.

An iteration on speed is required because several of the quantities used in calculating the work (i.e. valve pressure drop, electric motor heating, etc.) are themselves, directly or indirectly, functions of speed. This iteration is initiated by guessing the compressor speed, calculating the torque required, determining the speed that corresponds to that torque, and calling a convergence routine that will give a new guess of speed based on the old guess and the calculated speed. The iteration is complete when the guessed speed equals the calculated speed.

The amount of heat that is transferred to the refrigerant as it passes over the electric motor must be determined before calculating the compression work. This heat, due to the inefficiency of the motor, is found from the difference between the work (or power) supplied to the motor, WE, and the work supplied to the compressor, WA. The heat transfer results in a increase in the enthalpy of the refrigerant given by:

$$\delta H = WE - WA$$

where WE and WA are both per unit mass. Assuming the pressure drop across the motor is negligible, the state of the refrigerant before it enters the compression chamber can be reckoned. Notice that the work required by the compressor, WA, has not yet been calculated, therefore an assumed WA is used in the first iteration. WE is also calculated from this WA using the electric motor efficiency, EFFMTR:

$$WE = WA / \text{EFFMTR}$$

Currently, the motor efficiency is assumed to be 85% which is a representative value for a small AC induction motor.

The inlet and outlet valve pressure drops are calculated by assuming that the volumetric flow rate, VDOT, is proportional to the square root of the pressure drop, δP :

$$\text{VDOT} = \text{COEFF} * (\delta P)^{1/2}$$

The valve coefficient, COEFF, can be evaluated using VDOT and the pressure drop at design conditions. Design VDOT is found by dividing the design mass flow rate (specified by the design heat rate) by the inlet specific volume. Pressure drop at design is 1.5 psi and 4 psi for the inlet and outlet valves respectively. These pressure drops are based on results reported in a paper by Jacobs[2]. Then solving for the pressure:

$$\delta P = (\text{VDOT} / \text{COEFF})^2$$

where the volumetric flow rate, VDOT, is evaluated by:

$$\text{VDOT} = \text{EFFVOL} * \text{SP} * \text{DIS}$$

The displacement of the compressor, DIS, is given to the module as a parameter and the speed, SP, is given (as a guess) by the convergence routine.

The volumetric efficiency, EFFVOL, is found by taking the ratio of the actual volumetric flow rate to the maximum possible volumetric flow rate. VDOT is the actual volumetric flow rate but the maximum possible volumetric flow rate is the product of displacement and speed. Using polytropic relationships the EFFVOL can be reduced to [3]:

$$\text{EFFVOL} = (1+C-C*(P_{cd}/P_{cm})^{1/n})*(v_{i1}/v_{cm})$$

Clearance volume, C, is the difference between the maximum volume of the compressor and its displacement, and is provided to the module as a parameter. P_{cd} and P_{cm} are the high and low pressures within the chamber (after inlet valve and before the outlet valve). Here v_{i1} and v_{cm} are the inlet specific volumes before and after the inlet valve and n is the polytropic exponent, used because a polytropic relationship was assumed in the development of EFFVOL. The exponent is given by:

$$n = \ln(P_{cd}/P_{cm})/\ln(v_{cm}/v_{cd})$$

this equation is presented in more detail below. Once the volume flow rate has been determined the mass flow rate of the refrigerant, FRM, can be found from:

$$\text{FRM} = \text{VDOT}/v_{cm}$$

where v_{cm} is defined above. Notice again that FRM is a function of speed and will vary as the program iterates on speed.

Once FRM is calculated, the electrical power, WDOT, required by the compressor motor follows as:

$$\text{WDOT} = \text{FRM}*\text{WE}$$

Figure 1 shows the actual cycle within the compression chamber. PINLET and PEXIT are the pressures of the refrigerant before the inlet valves and after the exit valve. P_{cm} and P_{cb} are the pressures of the refrigerant inside the chamber during the intake process. P_{cc} and P_{cd} are the pressures after compression, during the exhaust process. These operating pressures within the compression chamber (P_{cc} and P_{cd}) are found from the PINLET and PEXIT by using the polytropic equations above.

The indicated work, WI, which is the boundary work done on the fluid, is the difference between the work done during the compression (process B to C) and the work done to re-expand the vapor left in the chamber due to the clearance volume (process D to A) after the exhaust process is complete. This difference is signified by the enclosed area on the process diagram (Figure 1). This area represents the indicated work and can be calculated by the following equation:

$$\text{WI} = \int VdP - \int VdP$$

where the above integrals can be evaluated assuming the compression and expansion process follow a polytropic path. The resulting equation is [4]:

$$WI = (n/n-1)(P_c*v_c)((P_c/P_c)((P_c/P_c)^{(n-1/n)}-1))$$

The pressures and specific volume correspond to the those in Figure 1. The polytropic exponent, n, is evaluated using the end points of the compression process in the polytropic process equation:

$$P_c*v_c^n = P_b*v_b^n$$

solving for n:

$$n = \ln(P_c/P_b)/\ln(v_b/v_c)$$

where again the pressures and specific volumes correspond to the those in Figure 1. Notice that in the development of the indicated work equation it was assumed that the polytropic exponent is the same for both the compression and expansion processes.

The total work of the compressor, WA, is the sum of the indicated work which is calculated as reversible boundary work and the irreversible work which results from mechanical inefficiencies. WA is calculated as:

$$WA = WI/EFFMEC$$

EFFMEC is the mechanical efficiency of the compressor which is determined from a mechanical efficiency vs. speed curve included in a table lookup. The medium-sized compressor curve, Curve M shown in Figure 2, was used in the table lookup [5]. Notice that the efficiency peaks around 40 Hz. This is because the contact friction losses are relatively constant with frequency so that at lower frequencies these losses represent a larger portion of the input power causing the efficiency to be low. At higher frequencies the fluid friction increases thereby causing the efficiencies to be lower. After WA has been calculated, the torque, TRK, is determined using the following equation:

$$TRK = (FRM*WA)/(2*\pi*SP)$$

The torque is nondimensionalized and used to find the nondimensional speed as in the simple module above. And again, the compressor speed is obtained by multiplying the speed by the input frequency. This is the calculated speed given to the convergence routine.

Once convergence is complete, the exit enthalpy can be found by adding WA, the increase in enthalpy of the refrigerant during the compression process, to the enthalpy of the refrigerant before it enters the compression chamber and after it passes over the motor. The exit pressure was given to the module as an input so that the property routines can be called using these two properties to find the exit state.

In order to compare this more detailed (polytropic) compressor with the simple isentropic model, the overall isentropic and volumetric efficiencies must be computed. The overall isentropic efficiency is calculated by finding the hypothetical outlet state based on a isentropic compression process. This is done using the inlet entropy and the exit pressure. The equation for isentropic efficiency, EFF, is:

$$EFF = (HISEN - HIN)/(HEXIT - HIN)$$

Where HIN and HEXIT are the inlet and exit enthalpy and HISEN is the exit enthalpy for an isentropic compression. Overall volumetric efficiency, ETAV, which is the actual volumetric flow rate (mass flow rate times inlet specific volume) divided by the maximum possible volumetric flow rate (displacement times speed) is calculated as follows:

$$ETAV = (FRM*VIN)/(DIS*SP)$$

where VIN is the specific volume at the inlet to the compressor.

After convergence is complete all the speed related quantities WA, WDOT, FRM, and etc., are set at the correct values for the given set of conditions. With these quantities and the outlet state, the main program can proceed to the condenser module.

2. Flow Control Device

The flow control device maintains a pressure differential between the condenser and evaporator. Conventional heat pumps rely on one of several practical devices for this function. The simplest component is a fixed restriction, normally a small diameter tubing or capillary. Controlled valves are typical in more contemporary applications. Both constant pressure and, most commonly, thermostatically controlled expansion valves are used.

In the current simulation program the expansion device is modeled as a simple capillary tube. This was done to make the initial simulation model as simple as possible while remaining physically realistic. Extension to a thermostatic expansion valve which would operate to maintain a set degree of superheat at the evaporator exhaust is straightforward and would entail the addition of a feedback control loop in the system. Since the control function would only serve to adjust the restriction between the condenser and evaporator, the development of a fixed-resistance capillary model was a necessary precursor. Various control strategies can be assessed once this extra complexity is included in the system. The possibility of direct digital control of the expansion valve by a microprocessor included in the heat pump's control system provides the opportunity to achieve optimal control of the pressure ratio to maximize the cycle COP or to help meet extreme loads.

The flow through a fixed expansion valve should be well into the hydraulically rough regime and, consequently, Reynolds number independent. This situation implies that the conventional valve coefficient model should be adequate. Using this formalism, the pressure drop is given by:

$$P_{\text{cond}} - P_{\text{evp}} = (V_r / C_v)^2$$

where V_r is the volumetric flow and C_v is the valve coefficient. The valve coefficient should be reasonably constant for a given device and refrigerant or even similar refrigerants. When the program advances to model controlled valves, the coefficient, C_v , will become a function of the valve opening.

Despite the complexity of attempting to model the flow of a two-phase and possibly accelerating fluid, the present fixed restriction model seems reasonably adequate. Some shortcomings are, however, apparent. In particular most of our simulations result in some vapor at the condenser outlet. We believe that this occurs because the simple one dimensional steady-flow model cannot simulate the actual separation of vapor and liquid that occurs in a condenser. The liquid in a physical condenser is sure to be precipitated and accumulated in a sump so that the expansion device will remain flooded with liquid. Our simulation implicitly assumes a one-dimensional flow so that this separation cannot be modeled. The continuing development of a transient condenser model should improve on this problem. We have also noticed that the conventional valve coefficient model may not be realistic in the laminar flow regime where a linear dependence between the pressure drop and the volumetric flow

is predicted along with a linear dependence on the viscosity.

While the present model appears to be adequate for system-level comparisons, we do plan further development of this model to allow for a controlled restriction. In addition, some investigation of the detailed fluid dynamics of this complicated flow seems indicated.

3. Simple Heat Exchanger Modules.

Two modules were developed to implement simple models of the condenser and evaporator. These modules have several uses including:

1. Expediting the development of the simulation system.
2. Providing preliminary results.
3. Serving as a system-level check on simulations that employ the more complicated modules.
4. Acting as prototypes for the more complicated modules.

In present form both modules consider only a single flow geometry, cross flow with the air side unmixed and the refrigerant side mixed. In their current form both modules appear to be reasonably accurate and numerically stable, but this level of performance has been attained only after considerable testing and development.

Our first attempt was at the development of an effectiveness versus NTU model. In the simplified modules variation in neither the air side nor the refrigerant side convection coefficients is currently considered; consequently, the overall conductance, "UA", is fixed. With the air flow specified as a function of the electrical frequency, the only unknown is the refrigerant heat capacity rate, C_r . This heat capacity rate can be calculated from the overall heat rate, Q , by:

$$C_r = Q/\delta T$$

where δT is the refrigerant temperature change. The heat rate can be calculated from the effectiveness, ϵ , by:

$$Q = \epsilon C_{\min} (T_h - T_c)$$

where C_{\min} is the minimum heat capacity rate and T_h and T_c are the hottest and coldest temperatures in either stream.

An obvious iteration loop is established by guessing a refrigerant heat capacity rate, using that value to compute the heat exchange effectiveness by standard analytical formulas, and then recomputing C_r from the resulting heat rate. This algorithm appeared to work rather well initially, but after further testing it was found to be numerically unstable. As discussed below this instability is manifested by simulation results being erroneously dependent on the initial guesses. This instability appears to be related to two fundamental problems. One is the vast range for values of the refrigerant

heat capacity rate. For a pure condenser or, more likely, a pure evaporator, C_r is infinite while for typical actual operating conditions it is only on the order of the air rate. The other problem is the nature of the thermodynamic property routines. Since the equation of state (PvT) is in virial form, unique and explicit results are obtained only when the independent variables are T and v. For other pairs, especially the combination of h and P which is ubiquitous in energy systems analysis, an iterative solution which must be slightly dependent on the initial guess is returned. A small perturbation in the thermodynamic state can cause a significant change in the computed heat capacity rate, and this is amplified by the strongly nonlinear dependence of the effectiveness on C_r .

Our initial attempt to address this problem was to switch to the use of the refrigerant temperature change rather than heat capacity rate as the iteration variable. This quantity is more tractable since it merely goes to zero for two-phase heat transfer rather than the infinite value for C_r . This change noticeably improved the stability of the simulation, but cases of non-unique convergence still occurred.

The successful solution to the convergence problem was the implementation of a more deterministic heat exchanger model that does not require iteration or unduly accurate determination of the change in the thermodynamic state. The exchanger is analyzed as a series (50 or 100) of elements. For cross flow, an element receives the entire refrigerant flow but only a fraction of the air flow; consequently, the air is sure to be the so-called "minimum fluid" for each element. The number of transfer units (NTU) can be calculated directly as

$$NTU = UA_j / C_{m,j}$$

where UA_j is the conductance for element j and $C_{m,j}$ is the air flow across element j. Since the refrigerant heat capacity rate greatly exceeds that for the air, the simple formula (valid for C_{min}/C_{max} equal to 0) is applicable so that:

$$\epsilon_j = 1 - \exp(-NTU)$$

The heat rate for an element is given by:

$$Q_j = \epsilon_j C_{m,j} (T_{air,in} - T_{ref,in})$$

where the two temperatures are the inlet air temperature and inlet refrigerant temperature (from the preceding element).

Since the maximum temperature difference must be between the fluids entering the element. The overall heat rate is accumulated by summing the elemental rates and the overall effectiveness can be computed from the definition

$$\epsilon = Q / Q_{max}$$

where the fundamentally limiting heat rate is given by:

$$Q_{\text{min}} = C_{\text{min}}(T_{\text{in}} - T_{\text{e}})$$

Since the heat rate would have already been evaluated deterministically, the minimum fluid can be selected and the effectiveness computed directly.

The heat exchange calculations are the most important and troublesome computations; however, it is also necessary to consider the air side fan dynamics. The fan laws are used to adjust the flow rate and hydraulic power for off-design conditions. Typically, a fan driven by an induction motor will operate within a few (2 to 5) percent of synchronous speed regardless of the load. It can be assumed then that the fan speed is a fixed fraction (near unity) of the synchronous speed. The flow rate at off-peak electrical frequency is given by:

$$V = V_{\text{d}}N/N_{\text{d}}$$

where V_{d} is the design volumetric flow and N_{d} is the design synchronous speed (e.g. 1200, 1800, or 3600 RPM) while V and N are the prevailing flow and speed. The synchronous speed is determined by the electrical design of the motor and the electrical frequency. Typically the indoor coil is provided with a centrifugal blower powered by a nominal 1/3 horsepower six pole motor (1200 RPM synchronous speed) and the outside coil is ventilated by an axial fan with a four pole motor (1800 RPM) of around 1/4 horsepower.

The hydraulic power of the fan (rate of flow work done on the air) varies with the cube of the speed ratio according to the appropriate fan law:

$$W = W_{\text{d}}(N/N_{\text{d}})^3$$

Design pressure drops are typically 0.3 inch (water gage) for the outdoor coil and about 0.8 inch for the indoor coil which serves a deeper coil and must accommodate the frictional resistance of the ductwork as well.

The electrical power consumed is typically much greater than the hydraulic power on account of the necessarily low efficiency of the small fans. This power is given by:

$$W_{\text{e}} = W/\eta_{\text{e}}$$

In heat pump applications the fans are typically mounted downstream to provide a favorable pressure gradient across and thereby a more uniform flow through the coils. The leaving air enthalpy is increased by the amount of electrical power consumed all of which can be assumed to be dissipated in the air stream. This configuration dictates that the indoor fan power augments the heating effect and reduces the cooling effect of the indoor coil. All power from the outdoor motor is dissipated to the environment in such a configuration.

The fan efficiency surely varies with operating conditions, especially speed, but due to paucity of reliable data a fixed value of 50% is currently being used.

While adequate for present purposes the simpler heat exchange modules could be improved by the following enhancements:

1. The fixed air-side convection coefficient is a detriment. This could be improved by using a simple Reynolds analogy formulation that in particular would account for the degradation in convection performance with reduced air flow.
2. If adequate experimental data can be obtained, an improved model for the fan efficiency should be developed. A functional relationship between fan speed and efficiency would be desirable.
3. The current geometry is pure cross flow. This is probably unrealistic for the indoor coil. Several passes should be allowed with the possibility of air side mixing between passes.
4. In these modules air is treated as a simple fluid with constant specific heat. The models should be enhanced to be compatible with the moist air thermodynamic model now under development.

4. Detailed Heat Exchangers

These modules contain two fundamental improvements with respect to the simple heat exchangers:

1. Variable convective heat transfer rates for both air (h_a) and refrigerant (h_r).
2. Correlations of experimental fan data with existing fan laws to generate predicted fan performance at adjustable speeds.

4.1 Condenser. The condenser (Figure 3) requires as input the refrigerant properties, the mass flow rate leaving the compressor, and the inlet air state and flow rate. The air is treated as an unmixed fluid while the refrigerant is considered to be a mixed fluid. In addition, all tube configuration, and geometric information are included as parametric inputs. The condenser consists of three sections which perform the heat removal from the refrigerant. These coincide with the three possible refrigerant states, superheated, two-phase and sub-cooled. Naturally the overall heat transfer coefficients (U) vary from section to section as well. Here U is based on the total air-side heat transfer area.

Because of the dependence of U on air-side area, the U_s in each section along with their respective areas must be known to calculate an overall UA for the condenser. The module proceeds from section to section until the total air-side area (A_{tot}) is allocated by keeping track of the sectional air-side requirements. These intermediary

areas are then designated "Ads", "Acon" and "Asc", corresponding to the desuperheating, condensing, and the subcooling areas.

These calculated areas affect the air mass flow rates directly thereby changing the minimum heat capacity rates needed for the effectiveness-NTU relations. While this module may be straight forward, many subroutines were needed to keep the appearance clean. A brief summary of the subroutines required by the condenser is given in the following list:

DESUP.....Calculates exit state (Hex) and Ads based on a variable Uds.

CONDENS...Calculates exit state (Hex) and Acon based on a variable Ucon.

SUBCOOL...Calculates exit state (Hex) based on remaining Atot and variable Usc.

CMCALC....Determines the fluid with the minimum heat capacity.

HOUT.....Called by DESUP & SUBCOOL to determine effectiveness, heat transferred (Q), and exit state (Hex).

AFIND.....Called by DESUP to calculate the area required to desuperheat the refrigerant.

FANCALC...Calculates the variable volumetric air flow rate, fan work and efficiency.

CALCNTU...Calculates the overall NTU's based on an overall effectiveness.

GEOM.....Calculates the major geometric heat exchanger parameters needed to determine h_m , h_r , and Atot.

U1.....Called by DESUP to calculate h_m , h_r , and ultimately Uds.

U2.....Called by CONDENS to calculate h_m , h_r , and ultimately Ucon.

U3.....Called by SUBCOOL to calculate h_m , h_r , Usc.

4.2 Evaporator. The evaporator (Figure 4) requires the indoor air state and flow rate, the refrigerant mass flow rate, the inlet refrigerant enthalpy, the "guessed" low-side pressure, and the "required" low-side or evaporator heat rate. As was the case with the condenser, the air is considered to be unmixed and the refrigerant mixed. Parametric inputs include the heat exchanger geometry. The main algorithm consists of an iteration to find the refrigerant state that provides the required heat rate via a first law analysis of the overall heat pump system ($QLR = W - QH$). The algorithm computes the low-side NTUs, the effectiveness, and the calculated low-

side heat rate, QL. The module then updates the low-side temperature (and hence pressure since the evaporator operates for the most part in the two-phase region of the refrigerant) based on a comparison with the required low-side heat rate:

$$TE = TA - [QLR/QL]*[TA - TEOLD]$$

where TE is the updated evaporator temperature, TA is the inlet air temperature, and TEOLD is the previous evaporator temperature.

The majority of heat transfer is two-phase boiling, so only one overall U needs to be calculated. Since the inlet enthalpy and QLR are fixed, iteration ceases when the appropriate saturation temperature and its corresponding pressure are found. The additional subroutines needed for this module are:

FANCALC...Calculates variable volumetric air flow rates, fan work and efficiency.

GEOM.....Calculates Atot and other major geometric parameters needed for UEVAP.

UEVAP.....Calculates ha, hr, and ultimately ULS (low side).

4.3 Description of DESUP, CONDENS, SUBCOOL. DESUP begins by determining the exiting enthalpy based on total allocation of Atot. This value is then compared to the saturated vapor enthalpy (h_g) at that pressure. If the calculated Hex is less than h_g , then too much area was used and AFIND is called to determine correct Ads and Hex. If on the other hand the calculated Hex is greater than h_g , then Atot is not an adequate amount of area to desuperheat the fluid, and the condenser computation is completed.

CONDENS assumes the entering state is saturated vapor at Psat. Via the effectiveness-NTU relations Qmax and the necessary Acon are calculated [6]:

$$\epsilon = 1 - \exp(-NTU)$$

$$Q_{max} = Q/\epsilon$$

where $Q = H_{r,g}$. If Acon is greater than Atot - Ads, then the actual exiting state will be within the two-phase region and Acon is set equal to Atot - Ads. If on the other hand the opposite is true, then this section will have an exiting state at saturated liquid (quality = 0) and the remaining area from Atot can be used to sub-cool the refrigerant.

At this stage the only area available, if any, for heat transfer is Atot - Ads - Acon. Given this area, SUBCOOL calculates Cmin, the NTUs, and the effectiveness. SUBCOOL is a virtual mirror image of DESUP operating in the liquid refrigerant region without the added difficulty of finding Asc.

4.4 Calculation of variable heat transfer rates. The convective heat transfer rate for air (h_m) is dependent on the heat exchanger geometry, flow arrangement, and the air flow rate. The correlations used in these modules largely reflect the flow configuration and geometry appropriate to evaporators and condensers. In this case the Oak Ridge model [7] was determined to be the most general and yet retain provisions for detailed analysis. With a few minor simplifications, the subroutine GEOM was written to supply the necessary parameters for the correlations used. These empirical formulas are given below.

For air, a single correlation was used and assumed constant through each section for a given fan speed [7]:

$$h_m = C_c * G_a * C_p * Pr^{-0.4} * J * ((1 - 1280 * Nt * Re^{-1.2}) / (1 - 5120 * Re^{-1.2}))$$

where $C_c = 1.45$ for wavy fins.

$Re = G_a * Wt / \mu$

$Fa = [\text{fin heat transfer area}] / A_{tot}$

$Wt = \text{Horizontal distance between tubes}$

$G_a = \text{Mass velocity based on free flow area}$

$J = .0014 + 0.2618(1/(1-Fa))^{-0.15} (G_a * D / \mu)^{-0.6}$

The refrigerant requires four correlations to account for the different heat transfer regimes. For a superheated refrigerant [7]:

$$h_r = C_1 * Gr * C_{p_v} * Pr^{-0.4} * Re^{C_2}$$

$C_1 = 1.10647$	$C_2 = -0.78992$	for $Re < 3500$
$C_1 = 3.5197(10)^{-7} C_2 = 1.03804$		$3500 < Re < 6000$
$C_1 = 0.0108$	$C_2 = -0.1375$	$Re > 6000$

For two-phase heat transfer a distinction must be made between condensing and evaporating. McQuiston [8] had the most compact versions while yet still relying on the geometry of the heat exchanger. For condensing:

$$Nu = 0.1 * Pr^{0.33} * [i_{fg} / c_p * \delta T]^{1/4} * [(D * G / \mu_L) * (\rho_L / \rho_v)^{-0.5}]^{0.66}$$

where i_{fg} = enthalpy of vaporization
 k = thermal conductivity
 μ = absolute viscosity
 δT = difference between T_{sat} and T_{wall} .

For evaporating:

$$Nu = C_1 * ((G * D / \mu_L)^n * (J * \delta x * i_{fg} * g_c / L * g))^n$$

where $C_1 = 9(10)^{-4}$ when $x_m < 0.9$
 $n = 0.5$ when $x_m < 0.9$
 δx = change in quality (assumed = 1.0)
 $J = 1$ when working in SI units
 $g_c = 1$ when working in SI units

The correlation used for a sub-cooled liquid was drawn from ORNL [7]:

$$h = 0.023 * Gr * Cp * Pr^{(C-1)} * Re^{-0.4}$$

where C = 0.3 when the refrigerant is being cooled. ASHRAE data [9] was used to calculate the temperature-dependent thermophysical properties of the refrigerant.

4.5 Modeling of Fan Performance. Subroutine FANCALC calculates the volumetric air flow rate, efficiency, and fan work as a function of frequency. Since these values are required for differing frequencies, some knowledge of the fan and system curves must be known at each frequency. While the system curve remains constant, the fan curves do not. With the aid of the fan laws [10] the general quadratic shape for these curves can be generated at any speed. This is demonstrated in Figure 5, where the curves for the system and fan curves are of the form:

$$H_{fan} = A - B * Vdot^2$$

$$H_{system} = C * Vdot^2$$

The constants A and B are determined from a fan manufacturer's equipment catalog [11], and the constant C is determined from a system requirement of approximately a 55 Pa pressure drop at an air flow rate of 0.5 m³/s.

While most of the initial barriers have been tackled, those remaining include the incorporation of the dehumidification in the evaporator, and the inclusion of a moist air thermodynamic property routine. Furthermore a series of vigorous simulations must be performed to test the validity of our results.

At this time the psychrometric algorithm has been written and needs to be coded and installed. To verify the results, trial runs will be performed and compared to similar runs generated the simplified versions. As we stand now, the results obtained appear to be reasonable, but more work needs to be done to verify this.

III. SIMULATION SYSTEM

1.0 Overview

The simulation system includes a main program, four component modules, and several utility programs. The main program manages the input of data, the output of results, and oversees the cycle convergence procedure. The component modules treat each of the four heat pump system components: the compressor, condenser, flow controller, and evaporator. The utility programs implement convergence procedures, compute thermodynamic properties, and perform numerical operations such as interpolation.

The primary function of the main program is supervision of the sequential, and iterative cycle analysis. The block diagram shown in Figure 6 illustrates the flow of information in the simulation system. If one chooses, as was done in this analysis, to begin the simulation sequence at the compressor inlet, guesses or initial estimates are needed for three quantities to allow the completion of the cycle analysis. These quantities are two properties of the refrigerant to fix its thermodynamic state and a guess of the condenser or high-side pressure which will allow the calculation of the refrigerant flow rate. Since guesses of three unknown quantities are required, iteration will be required until the guesses converge on calculated values. The information flow diagram (IFD) clearly illustrates the three information recycle loops that were used to analyze the heat pump system. Data supplied to a module are referred to as "inputs" and the results returned by a module are referred to as "outputs". These logical inputs and outputs frequently, but not always, correspond to the physical inlet (or intake) and outlet (or exhaust) quantities such as material flows and properties, heat rates, or control signals.

The compressor module requires values for the state of the inlet refrigerant (e.g. evaporator pressure, P , and suction enthalpy, h) and a value for the condenser pressure. These values cannot be known initially so reasonable guesses must be generated. With these inputs, the mass flow rate and outlet state can be computed as output variables. The condenser module requires the refrigerant mass flow and inlet state, the condensing or high-side pressure, and air properties. The inlet air properties are known from specification of the operating conditions. In the simple model, the fan laws are used to compute the air flow rate and fan power from rated conditions and a specification of the fan efficiency. Values for the refrigerant flow and state come from the compressor module. The condenser is followed by the flow control valve (FCV). The module representing the flow control valve computes a new value for the high-side pressure from the condenser outlet state and the evaporator pressure. Since the FCV output includes the recalculated value of a previously guessed value, this point in the IFD is a critical decision node for the innermost recycle loop. The convergence routine must compare the computed value with the guessed value and provide a new guess if the agreement is unsatisfactory.

Once a convergent value for the high side pressure has been found

for a particular guess of the compressor inlet state or suction state, the main program calls the evaporator module. The evaporator module computes its outlet state from its inlet state (h and P) and the mass flow rate. Steady state operation demands that for convergence the heat burden on the evaporator (condenser heat rate minus compressor power) equal the heat rate of the evaporator. Since the inlet air must be the highest temperature and the inlet refrigerant the lowest temperature in the heat exchanger, the heat rate is given by the usual effectiveness formula:

$$Q_{ev} = \epsilon C_{m,a,r} (T_{m,a,r} - T_{a,r})$$

where ϵ = evaporator effectiveness
 $C_{m,a,r}$ = minimum heat capacity rate
 $T_{m,a,r}$ = air inlet temperature
 $T_{a,r}$ = refrigerant inlet temperature.

Unless the guessed evaporator pressure was fortuitously accurate, the heat rate will not agree with the heat burden. A formula is needed to compute an improved guess of the evaporator pressure; lower if the heat rate is too small so that a colder evaporator is required and conversely if the heat rate is larger than the heat burden. Such a formula can be obtained by solving the preceding equation for the product, $\epsilon C_{m,a,r}$, and then applying the effectiveness formula for the heat burden, Q_r , but with an unknown refrigerant inlet temperature given. This inlet temperature is assumed to be the saturation temperature for the unknown evaporator pressure, and is given by:

$$T_{m,e,t} = T_{m,a,r} - (T_{m,a,r} - T_{a,r}) Q_r / Q_{ev}$$

The fluid at the evaporator inlet will be a two-phase mixture for all reasonable operating conditions. Consequently the newly calculated evaporator pressure is just the saturation pressure corresponding to $T_{m,e,t}$. Note that when the heat burden equals the heat rate the calculated $T_{m,e,t}$ will equal the prevailing inlet temperature, $T_{a,r}$. A recycle loop internal to the evaporator model to obtain a convergent value for the evaporator pressure speeds the system simulation.

The output of the evaporator module is a decision node for two recycle loops. One for the evaporator pressure and an outer loop for the suction enthalpy. In practice several iterations are usually required to obtain a convergent evaporator pressure whereas convergence for the suction enthalpy is quicker since the evaporator pressure has been adjusted to make the evaporator heat rate approximately match the heat burden.

2.0 CONVERGENCE ROUTINES

A given recycle loop is, in general, an implicit nonlinear equation which gives a calculated value of a recycle variable in terms of the parameters of the system (such as heat exchanger specifications and compressor characteristics), conditions of operation (including the

air side temperatures and electrical frequency), and other process variables some of which may be recycle variables in other subsidiary or superior recycle loops. A general representation of a recycle loop is simply:

$$X_c = F(X_g)$$

where X_c is the calculated value, returned from a component module and X_g is the guessed value, provided by an initial guess or by a convergence routine.

The easiest feasible convergence routine is probably just simple resubstitution such that the calculated value is used as the new guess. This procedure is sometimes reasonably efficient in inherently stable applications such as thermal resistance networks. However the highly nonlinear behavior of the heat pump system requires a more sophisticated approach.

The first procedure considered was Wegstein's method [12] which is illustrated in Figure 7. The implicit relationship is illustrated by the unknown curve labeled $F(X_g)$. Convergence is obtained when $X_c = X_g$, a condition represented by the straight line along the main (45°) diagonal. The first step of Wegstein's method is simple resubstitution such that:

$$X_{g2} = X_{c1} = F(X_{g1})$$

Note that the analyst must provide the initial guess in any event. Since a convergent solution is represented by a point on the main diagonal, the second and subsequent steps proceed by extrapolating from the last two points (A and B in the figure) to the main diagonal (point C). Analytically then the next guess is given by:

$$X_{g3} = (X_{g1}X_{c2} - X_{g2}X_{c1}) / (X_{g1} - X_{g2} - X_{c1} + X_{c2})$$

Wegstein's method works reasonably well with many ill-behaved functions but in the heat pump simulation some of the relationships are too extreme, and improved convergence procedures were necessary.

Possibly the most difficult convergence problem is the innermost recycle loop for which the recycle variable is the condenser pressure. A sketch of the dependence of the calculated condenser pressure, P_{cc} , on the guess of condenser pressure, P_{cg} , (for a given evaporator pressure and suction enthalpy) is shown in Figure 8. Note that a larger guessed pressure returns a low calculated pressure because in such a case the refrigerant is sure to be condensed at the higher operating temperature range. In contrast, a low guess of the condenser pressure causes the system to simulate low temperature heat exchange and a corresponding small heat rejection rate. This results in substantial vapor in the exhaust and an enormous increase in the pressure calculated by the FCV module.

Several approaches were attempted in an effort to deal with this problem. The most obvious problem with applying Wegstein's method is apparent in Figure 9. An initial guess of P_1 results in point A.

This is followed in the resubstitution step with a new guess of P_{in} which returns point B. Projection on the main diagonal results in the improved guess of P_{in} resulting in point C. Point C is followed by another improved guess at point D. So far the method is approaching convergence but the next guess will be the projection of the last two points which are now C and D. Their projection results in a guess such as P_{in} with which the procedure begins to diverge. Wegstein's method therefore is unsuited for relationships such as this high-side pressure curve.

In attempting to deal with the preceding problem, it was observed that the high-side pressure curve is basically convex so that improved projections always result when the new guess is based on the projection on the main diagonal between the last two points on opposite sides of the diagonal. In the preceding example the projection between D and C should be deferred in favor of using the projection between D and B, the last opposing points. Applying this procedure would yield the improved guess, P_{in} . A subroutine called CONVX was written to implement the procedure, and in some cases it was able to handle the high-side convergence problem.

In general however, difficulties persisted. It was found that for some conditions of operation no convergent high side pressure was returned by the convergence routine CONVX. This is an unexpected result since the procedure would have already found an interval containing the solution and would only continue to reduce the width of the interval as the procedure progressed. A detailed numerical investigation was conducted, and it was found that for some values of the outer recycle variables convergent values for the calculated high-side pressure were not necessarily obtained even when the width of the convergent interval was reduced to the limits of accuracy in the floating point arithmetic on our main frame computer. Apparently, this situation is caused by some inherent inaccuracy in the thermodynamic properties routines.

A practical solution to the high-side convergence problem was found by employing a modified interval-halving technique. This procedure begins with resubstitution steps until sequential points are found which are on either side of the main diagonal. Once this convergent interval is identified, a simple interval-halving procedure is instituted. It is no longer necessary to find a guessed pressure that returns a nearly equal calculated value but only to reduce the width of the convergent interval to an acceptable value. This procedure is reasonably efficient and very stable as it invariably results in an accurate high-side pressure.

This procedure implemented by subroutine CONRHAV, for convergence by resubstitution and halving, has also been used successfully for the less challenging outer recycle loops.

3.0 Utility Routines

Several important utility routines are used in the simulation system for evaluation of the thermodynamic properties of the refrigerant and for numerical procedures including interpolation of tabulated data.

The thermodynamic properties routines are based on Reynolds [1] who presents valid formulas for the superheated vapor region. The formulation used for the refrigerants is based on a virial equation of state (explicit in the density, p , and the temperature) having the general form:

$$P = RT\rho + F(T, \rho)$$

The equation of state data is complemented by low-density, or ideal-gas state, specific heat data. The P ρ T data can be combined with the ideal-gas specific heat data in the standard fashion to yield an expression for the internal energy of the form:

$$u = c_v dT + \int [1/\rho^2][P - T(dP/dT)_{\rho}]d\rho + u_0$$

The entropy can be obtained in a similar fashion, and the enthalpy can be evaluated from its fundamental definition, $h = u + Pv$. The preceding equations are valid in the vapor region, including the saturated vapor. The formulations are, however, explicit in the independent variables T and v which are seldom convenient in energy systems analysis. An iterative procedure, also coded by Reynolds, has been used to evaluate the thermodynamic state in terms of other pairs of independent variables such as h and s and the most common pairing in energy systems analysis h and P . This procedure basically involves specifying the independent variables and making an initial guess of T and v if either is not specified followed by iteration until the specified independent variables are returned. Inaccuracy in the iteration procedure seems to be at the source of many of the numerical difficulties encountered while developing the simulation programs.

The preceding formulation is valid in the vapor phase only. To extend into the two-phase region requires vapor pressure data and a formula for the specific volume or density of the saturated liquid. Equations of the form $P_{sat} = F(T)$ are presented for the saturated vapor pressure curve. The evaluation also provides a value for the slope of the vapor pressure curve. The typical application begins by determining the saturation pressure from the temperature or the saturation temperature from the pressure by an iterative technique. The resulting pair of otherwise dependent variables still serve to evaluate the properties (h , u , s , and v) of the saturated vapor. Once the density of the saturated liquid has been determined, the specific volume change in vaporization, $v_{fg} = v_g - v_f$, can be computed and used in the Clapeyron equation along with the slope of the vapor pressure curve to evaluate the enthalpy of evaporation:

$$h_{fg} = Tv_{fg}(dP/dT)_{sat}$$

The entropy of evaporation is simply:

$$s_{rg} = h_{rg}/T$$

Having established the enthalpy and entropy of evaporation along with the density of the saturated liquid, the remaining saturated liquid properties are readily evaluated.

Evaluation of the thermodynamic properties can be extended into the slightly compressed liquid region by using the usual incompressible liquid model (i.e. $u = u(T, \text{only})$ and $v = v_r$).

Various auxiliary utility subprograms have been written to systematize the evaluation of certain thermodynamic properties. These include the following:

CALTV.....to calculate temperature and specific volume (in any phase) from h , P , and saturation properties.

PR12HP.....to calculate remaining properties (in any phase) given h , P , and saturation properties.

PSATP.....to determine the saturation properties as a function of pressure.

Other utility routines currently employed include a table lookup system from the Boeing MSF library published by the Control Data Corp. This system includes a search routine to locate the tabulated data nearest to the desired value of the independent variable or variables and then employs a Lagrangian interpolation technique to estimate the dependent variable at the desired point. The routine is flexible in the degree of interpolation allowed and can handle up to three independent variables.

Some further necessary or desirable work on the utility routines can be identified. Possibly the highest priority should be the improvement of the iterative thermodynamic properties routine. More accurate and, if possible, uniquely convergent solutions for independent property pairs other than T and v would be the goal. It would also be desirable to implement a non-proprietary table lookup system. Such a system tailored to the needs of a simulation program could be simpler and more efficient than the current system besides being transferable.

IV. ANNUAL BIN CALCULATIONS

1. Description

In order to compare the annual performance of the variable speed heat pump (VSHP) and the constant speed heat pump (CSHP), a simple method using temperature bins is used. Basically, a file contains the number of hours per year the ambient conditions are within temperature intervals or bins (the average temperature is used out of an interval of 5 °F) as shown in Figure 10 [13]. This file is used in conjunction with steady-state runs of the CSHP and the VSHP at these ambient conditions.

The hourly heat rate required is:

$$Q_{b_i} = UA [T_{r_i} - T_{a_i}]$$

where Q_{b_i} = Heat rate of the CSHP
 UA = Building conductance
 T_{r_i} = Balance point temperature
 T_{a_i} = Ambient temperature.

We selected a balance point temperature of 65 °F which accounts for internal heat generation. For small to moderate loads, the heat rate of the CSHP is determined by the ambient temperature T_{a_i} :

$$Q_{c_{i,cs}} = f(T_{a_i})$$

where $Q_{c_{i,cs}}$ is the heat rate of the CSHP and the portion of the hour it runs is given by:

$$t = Q_{b_i} / Q_{c_{i,cs}}$$

The CSHP will consume electric energy for this bin in the amount:

$$W_{c_i} = Q_{b_i} (1 \text{ hour}) / \text{COP}_{c_{i,cs}}$$

If $Q_{b_i} > Q_{c_{i,cs}}$, resistance heat has to be added:

$$W_{r_i} = (Q_{b_i} - Q_{c_{i,cs}}) 1 \text{ hour}$$

And the total electric energy consumed by the CSHP is:

$$W_{c_{i,cs}} = W_{c_i} + W_{r_i}$$

For moderate loads, the VSHP will run the entire hour but at a lower speed and presumably a higher COP to just meet the load:

$$Q_{b_i} = Q_{v_{i,vs}}$$

where $Q_{v_{i,vs}}$ is a function of ambient temperature and electrical frequency. The VSHP will consume a smaller amount of electrical power given by:

$$W_{v_{i,vs}} = Q_{b_i} (1 \text{ hour}) / \text{COP}_{v_{i,vs}}$$

Note that at very light loads, the VSHP cannot run the whole hour since minimum speed constraints will restrict the operation of the machine. A minimum frequency is imposed on the machine and if the heat load supplied by the VSHP is still too large for the house load, the VSHP will cycle on/off like the CSHP, but at a slower rate. At high loads, a maximum frequency limit is imposed on the VSHP; if the VSHP cannot meet the load when running at that maximum frequency, resistance heat is added as done for the CSHP. Also, only heating loads are considered and bins above 65 °F have been disregarded.

The program operates as follows:

1. Read the bin data, the CSHP data, and the VSHP data. The CSHP data consists of the results of several runs of the heat pump model running with an inverter efficiency of 100% and with a preset line frequency of 60 Hz for outside temperatures varying between 10 °F and 70 °F. The VSHP data consists of the results of several runs of the heat pump model running with an inverter efficiency of 90% and with inverter frequencies varying between 20 and 60 Hz and ambient temperatures varying between 10°F and 70°F. Also, two sets of runs were performed, one with the fans connected directly to the line at 60 Hz (fixed fan speed) and another with the fans connected to an inverter modulating their speed below 60 Hz.
2. Calculate the bin heat load, Q_b , based on house UA and ambient temperature.
3. For the CSHP, find through a table lookup procedure, the load supplied by the CSHP and its COP at a specific ambient temperature. If the bin load is smaller than the calculated Q_b , find the amount of time per hour the CSHP is operating. Here Q_{cs} is the heat supplied by the heat pump. If the CSHP cannot supply the load, add resistance heating.
4. For the VSHP, use the bin heat load and ambient temperature to find the appropriate inverter frequency. If the frequency is less than minimum, run the VSHP at minimum frequency, and supply the difference in resistance heat. Allow the VSHP to over speed up to 100 Hz. Above that frequency, cycle the machine on and off. Using the appropriate frequency and the bin temperature, find the COP and heat load Q_{vs} for the VSHP.
5. For both cases, Q_{cs}/COP gives the electric work required by the machine. Additional resistance heating is added if necessary to the cycle to give the total electric consumption.
6. These calculations are repeated for every bin temperature, multiplied by the number of hours in the bin and

summed to give total annual performance.

Note that cycling losses are not taken into account. Research indicates that these can account for a large decrease in performance since on and off switching of the compressor leads to high startup loads and shorter lifetime for the unit [14]. Cycling will usually affect only the CSHP since it cannot run at part load. The VSHP has to be properly sized to avoid cycling.

2. Results

The results will be discussed in two sections: one dealing with the results from the multiple program runs of the heat pump model, and one with the results of the BIN program.

In order to validate the model, several runs were performed with the ambient temperature varying from 10 °F to 70 °F. Figure 11 shows the comparison of the COPs of the conventional heat pump with the variable speed heat pump running at 60 Hz. Basically, the conventional heat pump COP curve runs parallel to the variable speed COP curve, with a 10% higher value. This is due to the inverter losses incorporated in the variable speed heat pump model which has an efficiency of 90%.

Figures 12 and 13 show the variation of the COP with frequency and ambient temperature for fixed speed and variable speed fans respectively. We chose to make this distinction because the power consumption of the fans grows proportionally to the cube of the fan speed which is always close to the electrical frequency (within 2 to 5%). In both the fixed speed and variable speed fan models, the fans operate at 60 Hz if the heat pump is running at a frequency higher than 60 Hz; the fixed speed fan runs continuously at 60 Hz, whereas the variable speed fan is connected to an inverter, and reduces its speed with the speed of the heat pump. The two figures show that the COP increases when the frequency is reduced. The curves display a different behavior depending on the ambient temperature, but basically show a maximum between 20 and 40 Hz. The fixed fan speed curves show a clear maximum at 30 Hz, with a degradation at lower frequencies. Both figures show a drop in COP at high frequency and high ambient temperature which indicates that the heat pumps should not be oversped significantly. Figures 14 and 15 show the same curves with the temperature in the abscissa instead of the frequency. The COP is much less sensitive to variations in outside temperature than to frequencies. It becomes more sensitive to the temperature if the frequency is lowered. This sensitivity is highlighted in the fixed fan speed figure which shows that at 20 Hz frequency, the curve as a function of temperature has changed so drastically that it crosses previous curves corresponding to higher frequencies.

The variation of the heat produced by the heat pump, Q_{h1} , shows a much more uniform behavior (Figures 16-19). Q_{h1} increases with increase in frequency and with increase in ambient temperature. The effect of the fixed or variable speed fan is not significant, and at 120 Hz, the curves show a cutoff in the amount of heat delivered

when the ambient temperature is above 50 °F.

These figures therefore give the range of operating conditions of the variable speed heat pumps, whether running with fixed speed or variable speed fans. The bin calculations take this fact into account. The variable speed heat pump does not operate at a frequency below 30 Hz or above 100 Hz.

The bin calculations show an overall annual energy consumption as a function of percent of load satisfied. The heat pump model simulates a 3 ton heat pump. The load of the house is varied so that the heat pump delivers the total heating load at peak conditions, or at a part load. Overall, the fixed speed fan model showed an improvement on the order of 8 to 10 percent over the conventional model, whereas the variable speed fan showed an improvement of 6 to 8 percent. Figure 20 shows the amount of annual electric resistance heat added to the heat pump models to satisfy the house load. As previously mentioned, this improvement does not consider the cycling losses which could be significant.

V. FUTURE WORK

The following items are identified as important tasks for continued model development and for the proper assessment of the energy and cost advantages of the variable speed drive heat pump:

1. Integrate and test the newly-developed heat exchanger models that incorporate variable heat transfer coefficients and variable speed fan characteristics.
2. Establish realistic performance parameters for the simulation code. Accurate parametric information is needed for the inverter, compressor mechanical efficiency, fan efficiency, and small motor efficiency. American and Japanese manufacturers' literature will be consulted as well as the results of the Georgia Power sponsored compressor testing component of this program.
3. Introduce the moist air thermodynamic property model and incorporate cooling and dehumidification in the evaporator coil.
4. Continue and complete the development of the transient version of the heat pump simulation code. Several important physical phenomena can be modeled only with transient effects included. System start-up and frosting are two such effects.
5. Perform simulation studies to ascertain the true advantages for the variable speed heat pump based on the more realistic modules discussed above.
6. Perform simulation studies to develop optimal control strategies for the operation of the variable speed heat pump. Included as control variables are the compressor speed, both fan speeds, and the operation of the flow control valve.

VI. REFERENCES

1. W. C. Reynolds, Thermodynamic Properties in SI, Stanford University, Stanford CA, 1979.
2. J.J. Jacobs, "Analytical and Experimental Techniques for Evaluating Compressor Performance Losses," Proceedings of the 1976 Purdue Compressor Conference, p 116, Purdue University, 1976.
3. J. L. Threlkeld, Thermal Environmental Engineering, Prentice-Hall, Englewood Cliffs NJ, 1962.
4. W. F. Stoecker, Refrigeration and Air-Conditioning, McGraw-Hill, New York, 1958.
5. E. Sakurai, "Measurement of Operating Conditions of Rolling Piston Type Rotary Compressors," Proceedings of the 1982 Purdue Compressor Conference, p 60, Purdue University, 1982.
6. W. M. Kays and A. L. London, Compact Heat Exchangers, 2nd ed., McGraw-Hill, New York, 1964.
7. S. K. Fischer and C. K. Rice, "The Oak Ridge Heat Pump Models: I. Steady-State Computer Design for Air-to-Air Heat Pumps," ORNL/CON-80/R1, Oak Ridge National Laboratory, Oak Ridge, TN 1980.
8. F. C. McQuiston and J. D. Parker, Heating, Ventilating, and Air Conditioning, 2nd ed., Wiley, New York, 1982.
9. "Thermophysical Properties of Refrigerants", ASHRAE, Atlanta, GA 1976.
10. ASHRAE Handbook of Equipment, ASHRAE, Atlanta GA, 1983.
11. A. Blackshaw, private communication, 1986.
12. R. F. G. Franks, Modeling and Simulation in Chemical Engineering, Wiley Interscience, New York, NY, 1972.
13. ASHRAE Handbook of Fundamentals, ASHRAE, Atlanta GA, 1985.
14. W. A. Miller, "The Laboratory Evaluation of the Heating Mode Part-Load Operation of an Air-to-Air Heat Pump," ASHRAE Transactions, 91, Part 2, 1985.

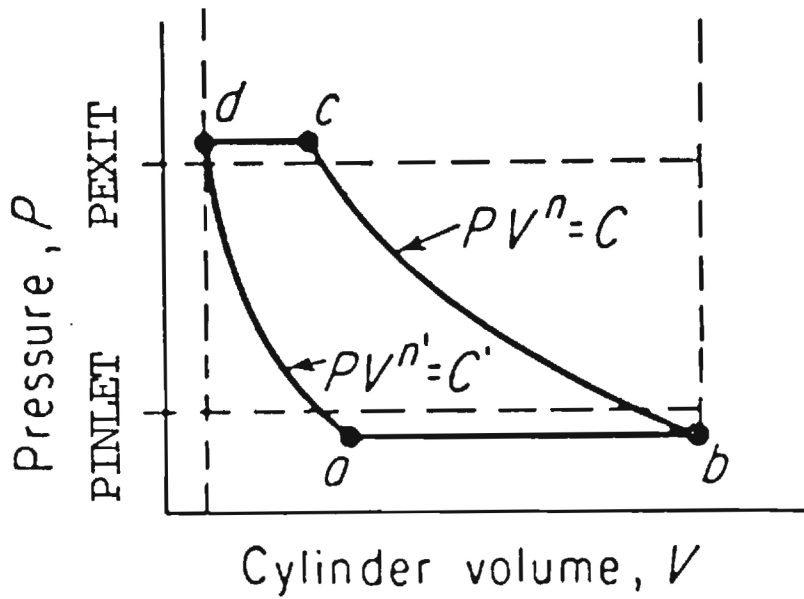


Figure 1.

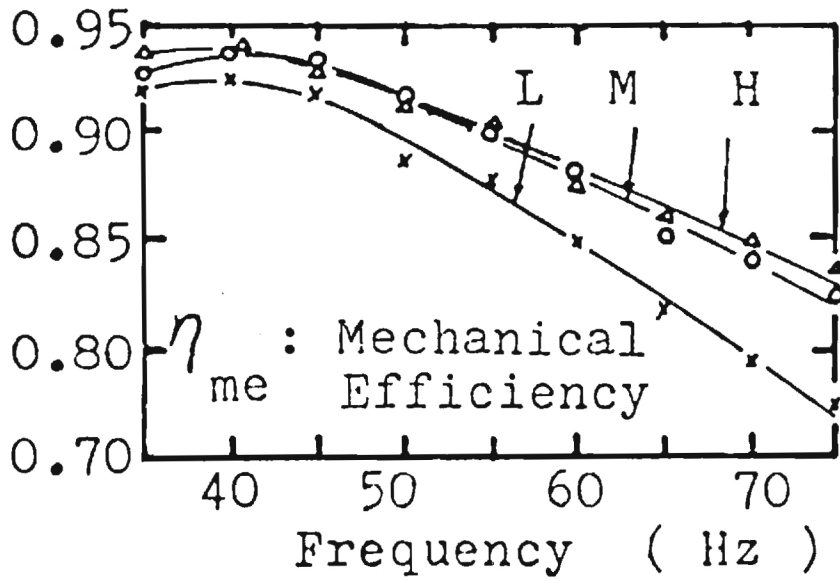


Figure 2

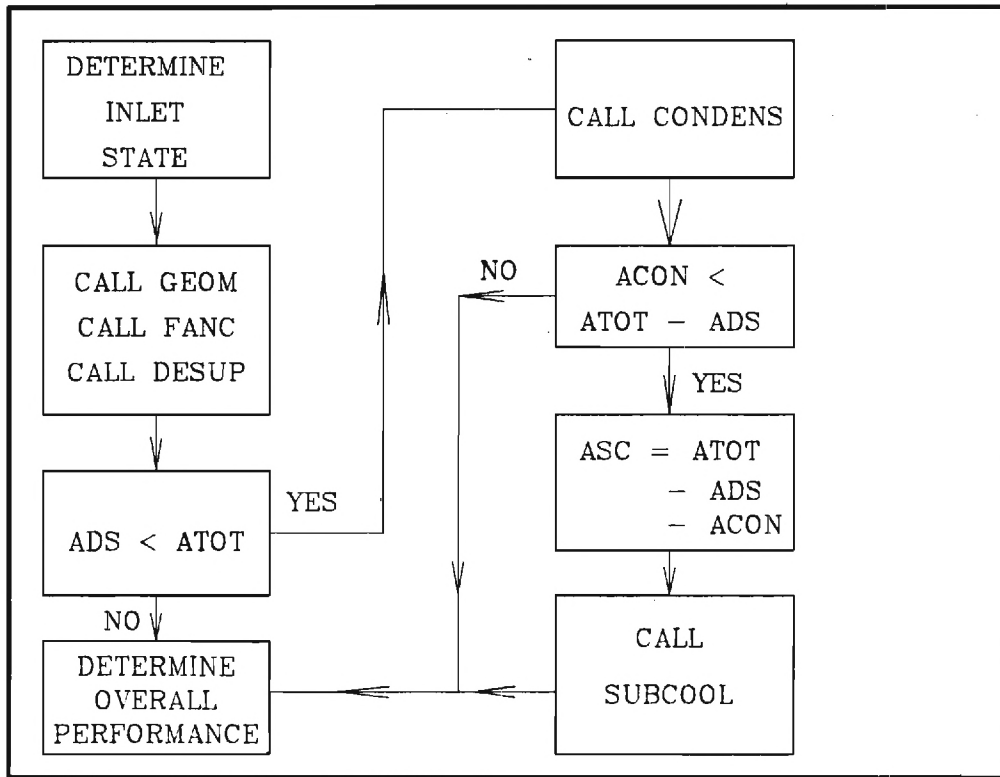


Figure 3

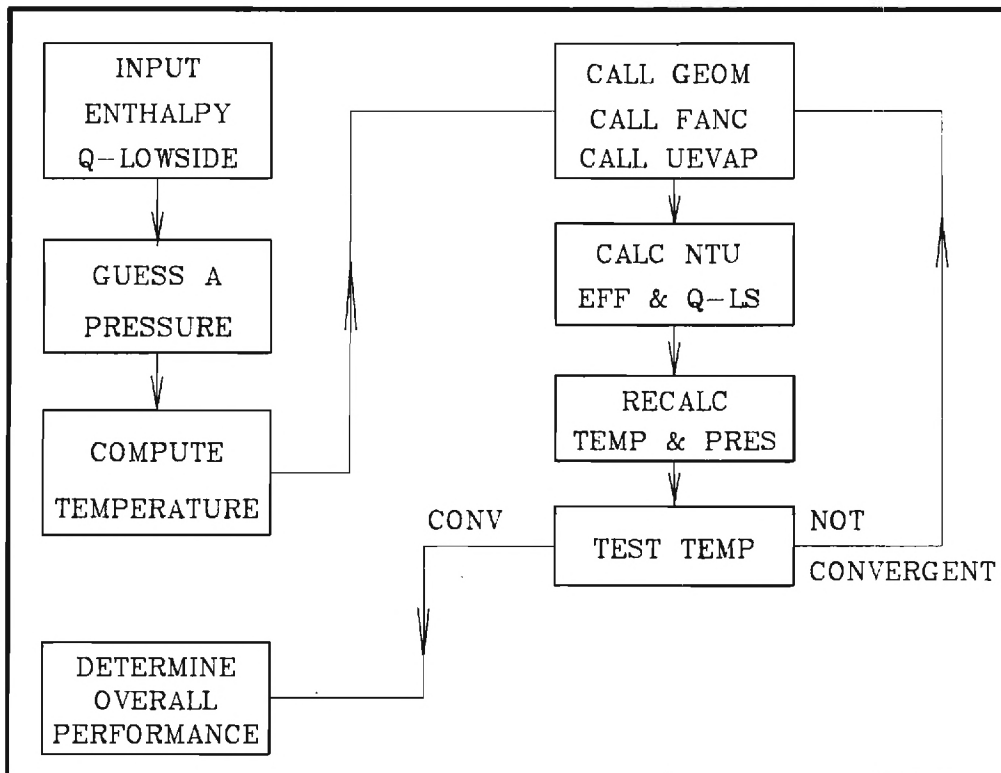


Figure 4

VARIABLE SPEED FAN CURVES

Hfan vs Hsystem (AAD,5/29/B6)

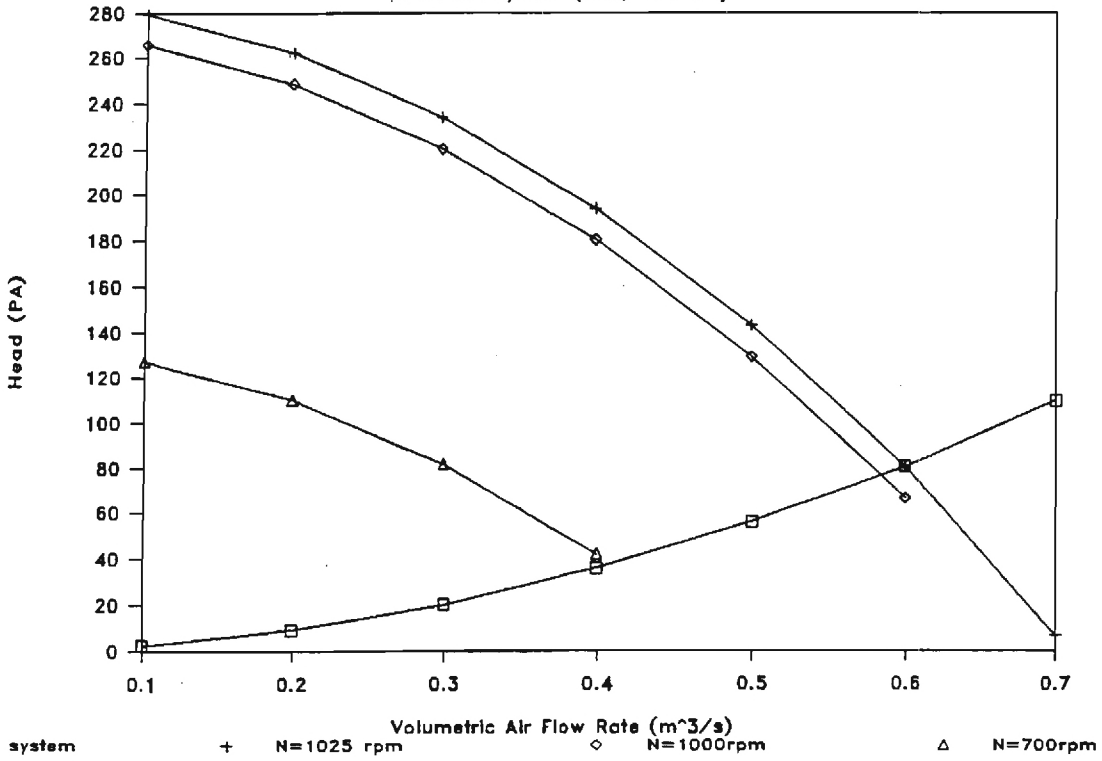


Figure 5

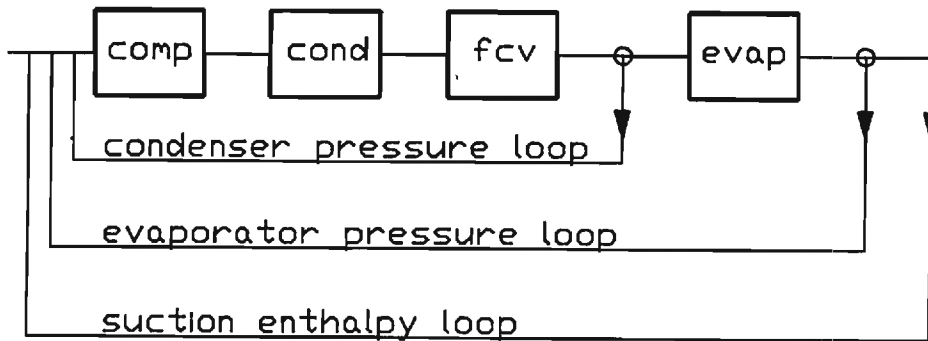


Figure 6

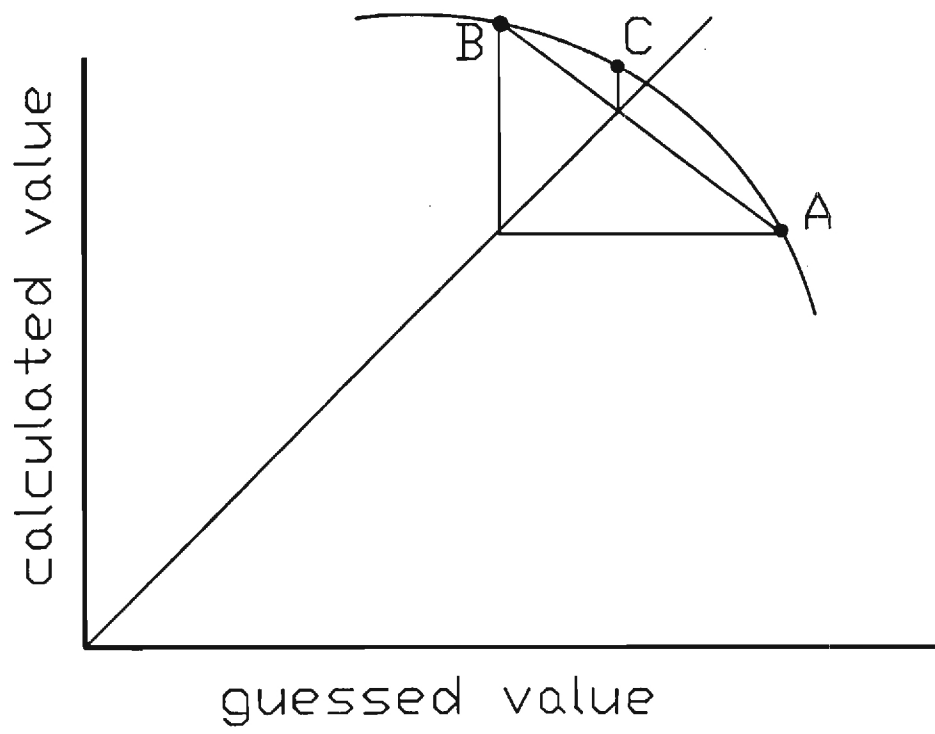


Figure 7

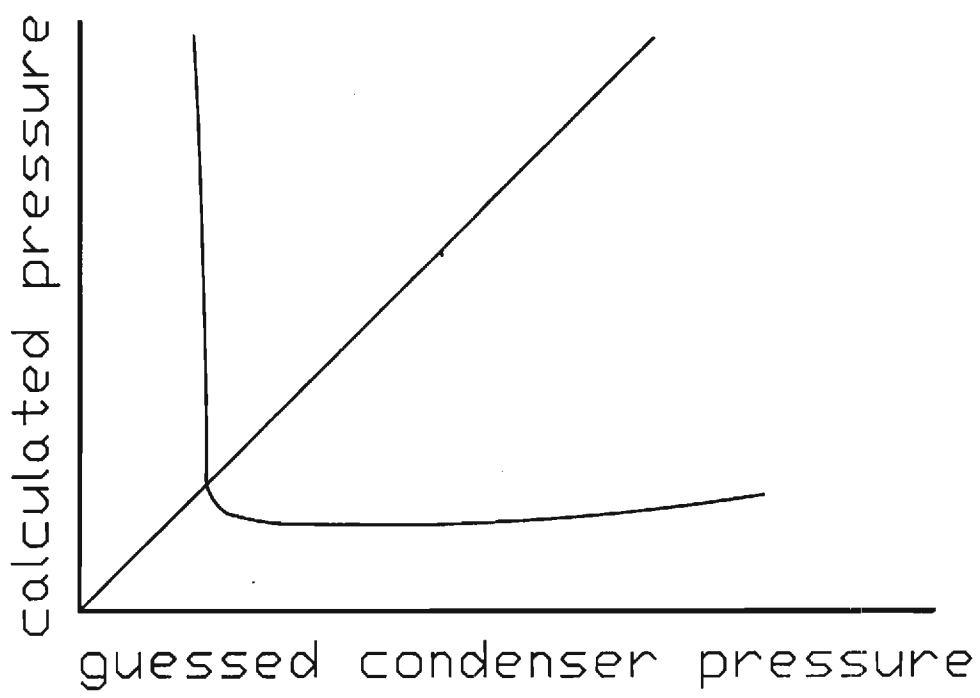


Figure 8

Comparison of C.O.P.'s

Conventional vs Variable Speed HP

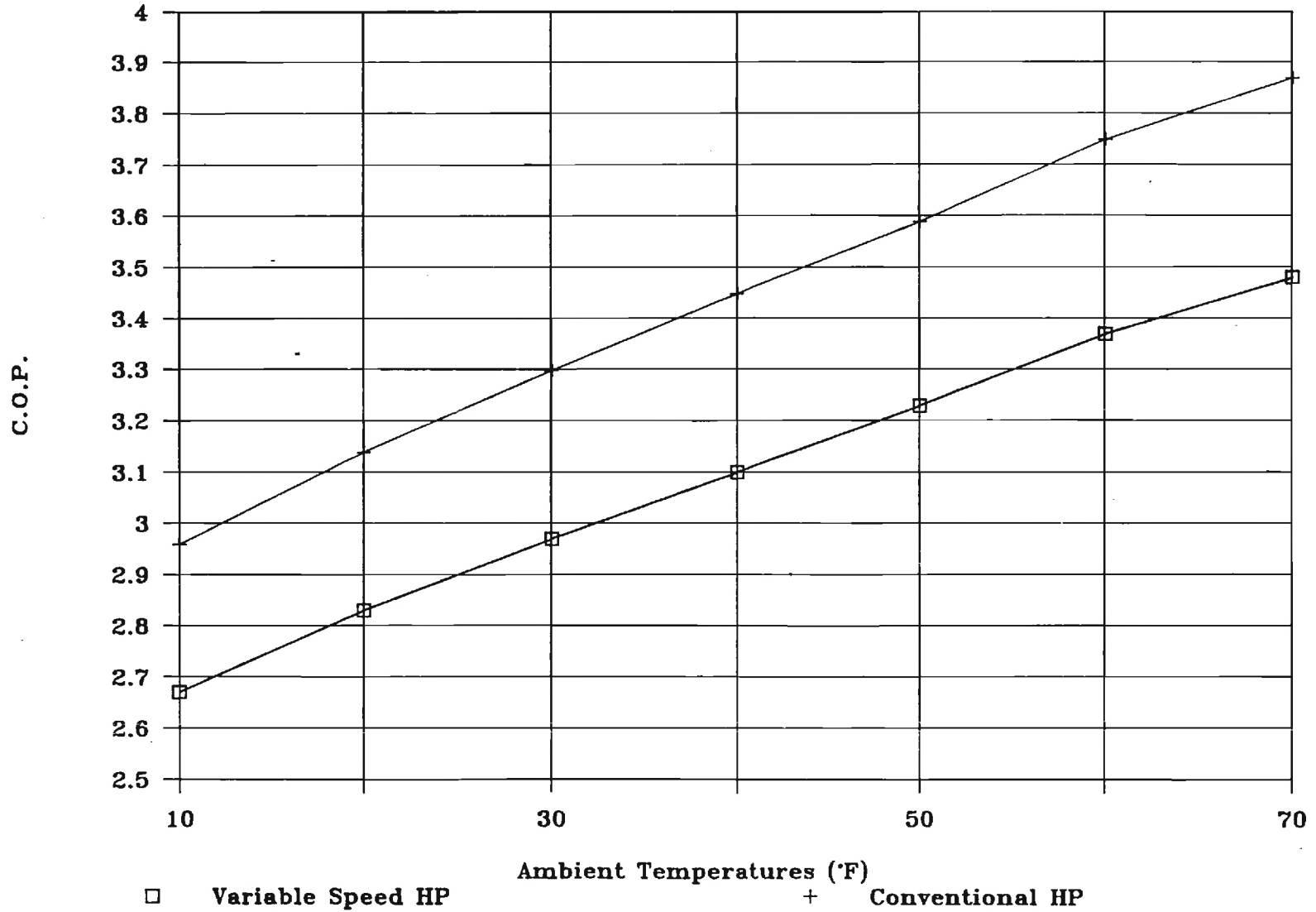


Figure 11

Variation of C.O.P.

Fixed Fan Frequency (60 Hz)

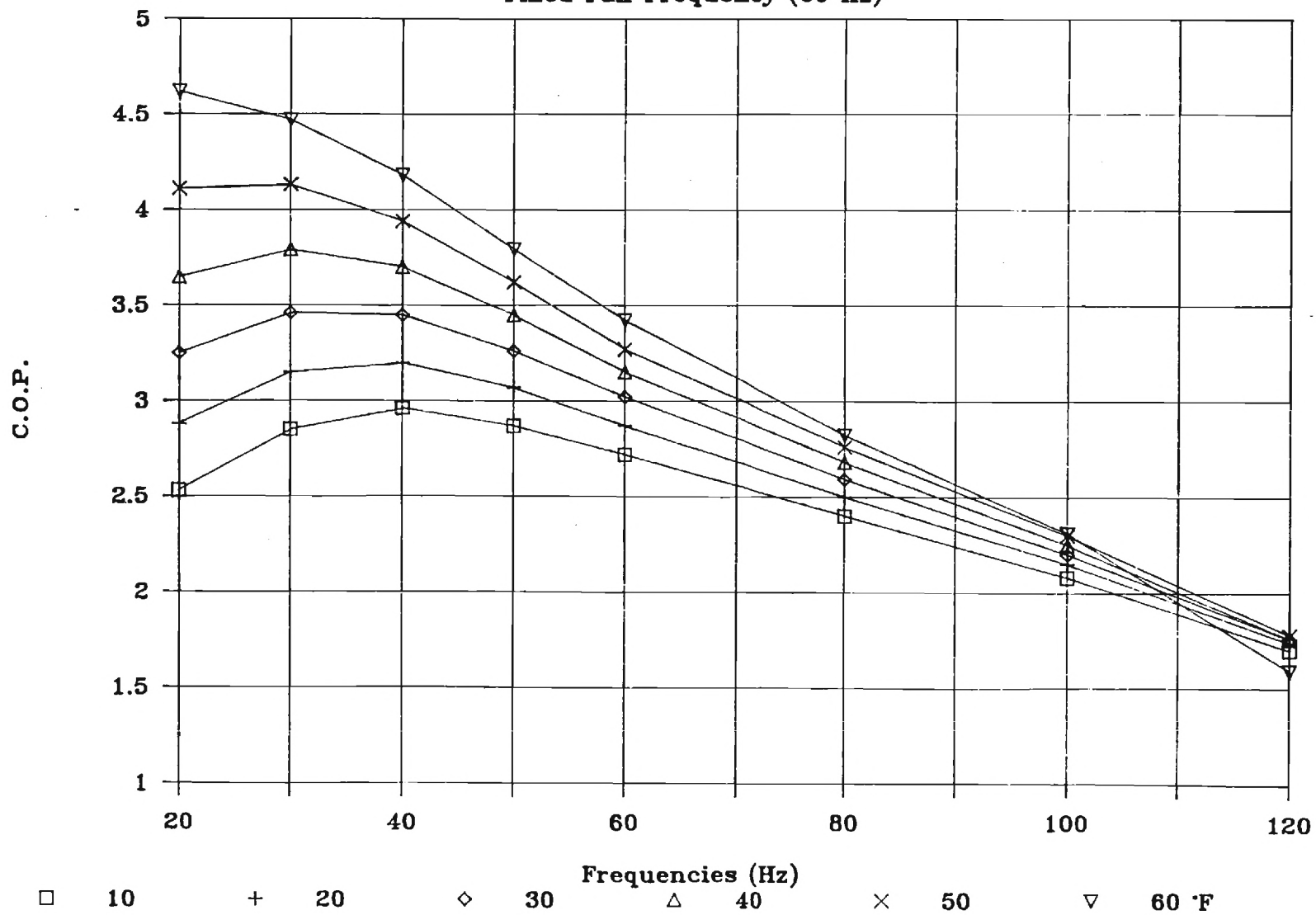


Figure 12

Variation of C.O.P.

Variable Fan Frequency (up to 60 Hz)

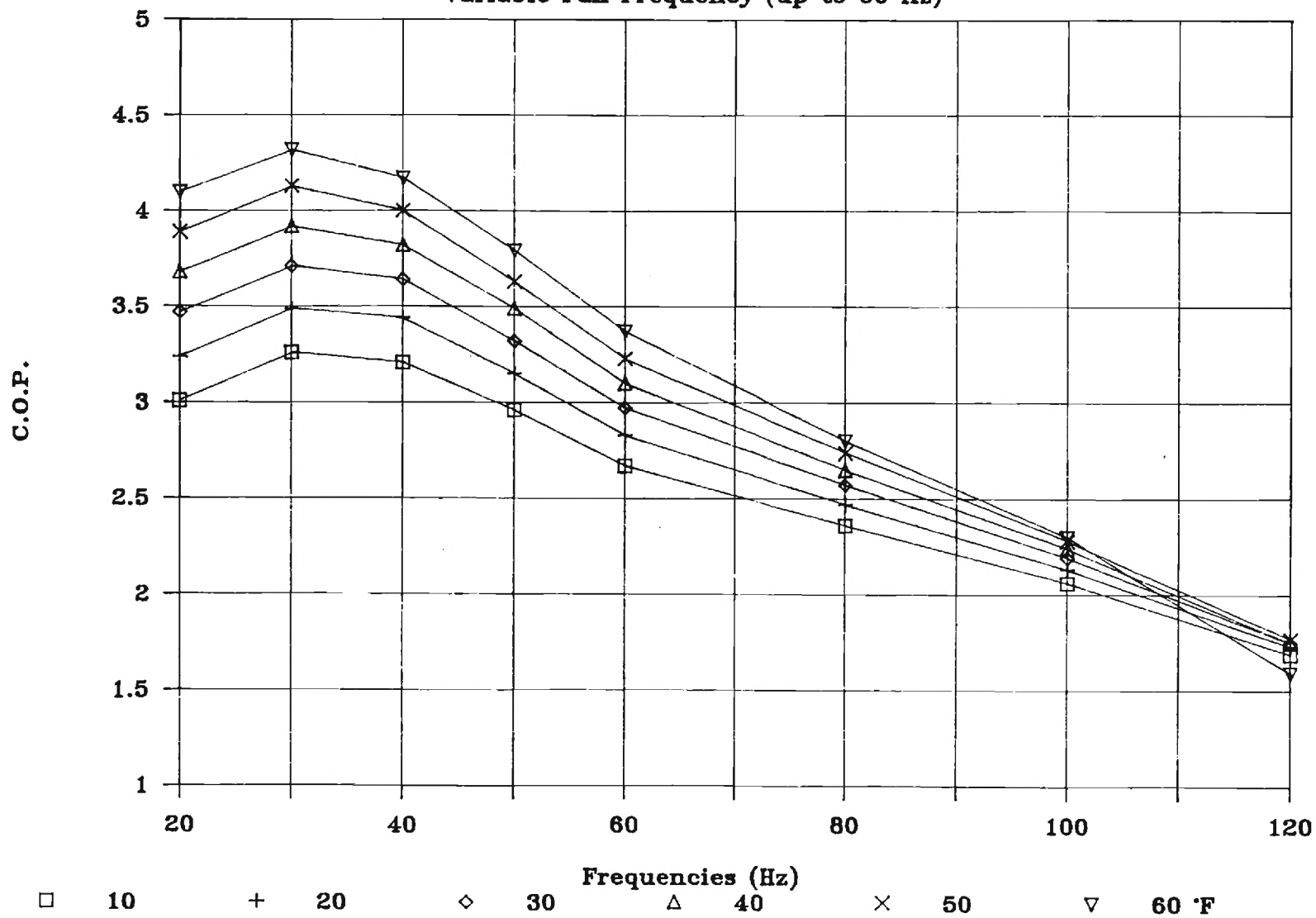


Figure 13

Variation of C.O.P.

Fixed Fan Frequency (60 Hz)

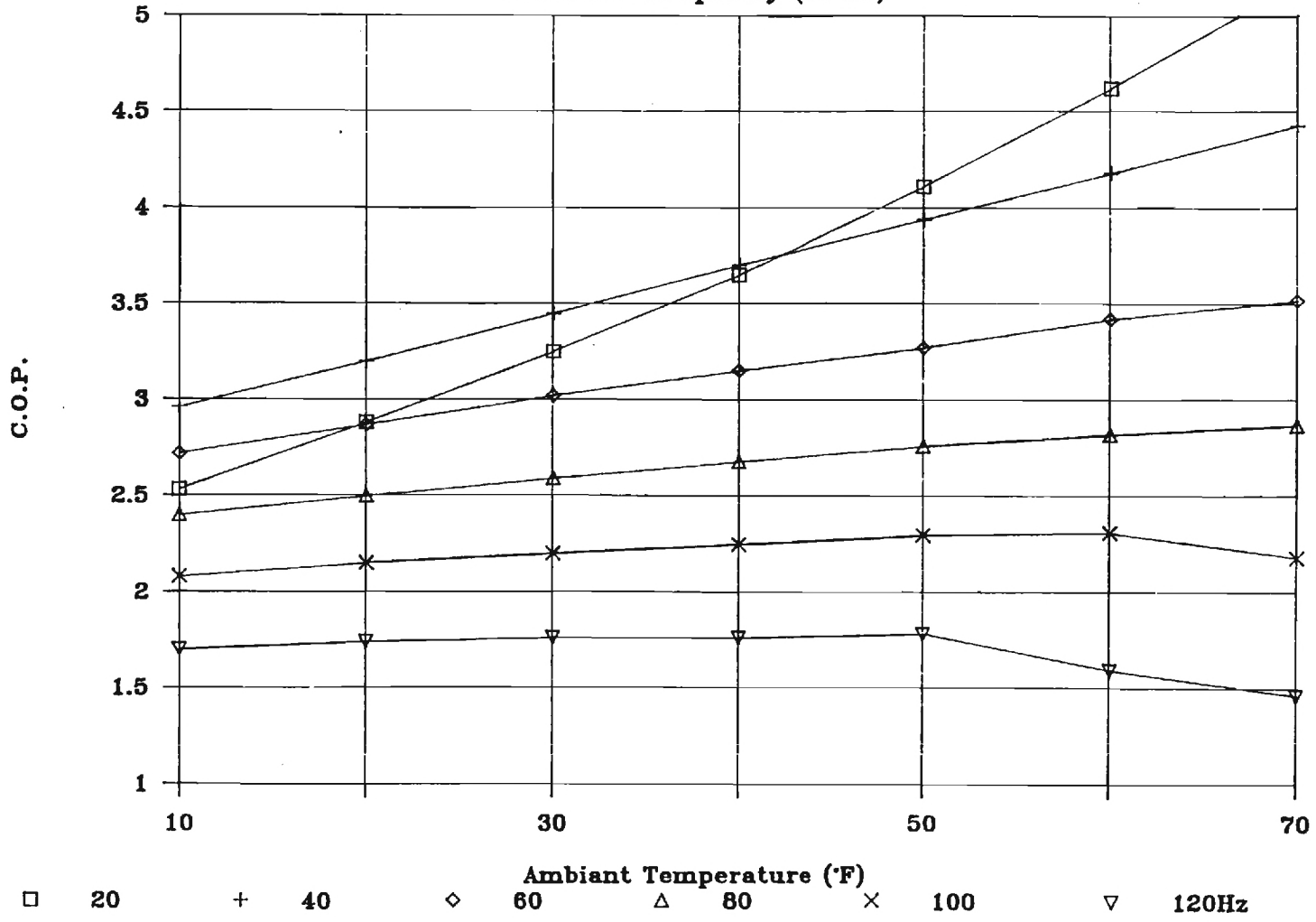


Figure 14

Variation of C.O.P.

Variable Fan Frequency (up to 60 Hz)

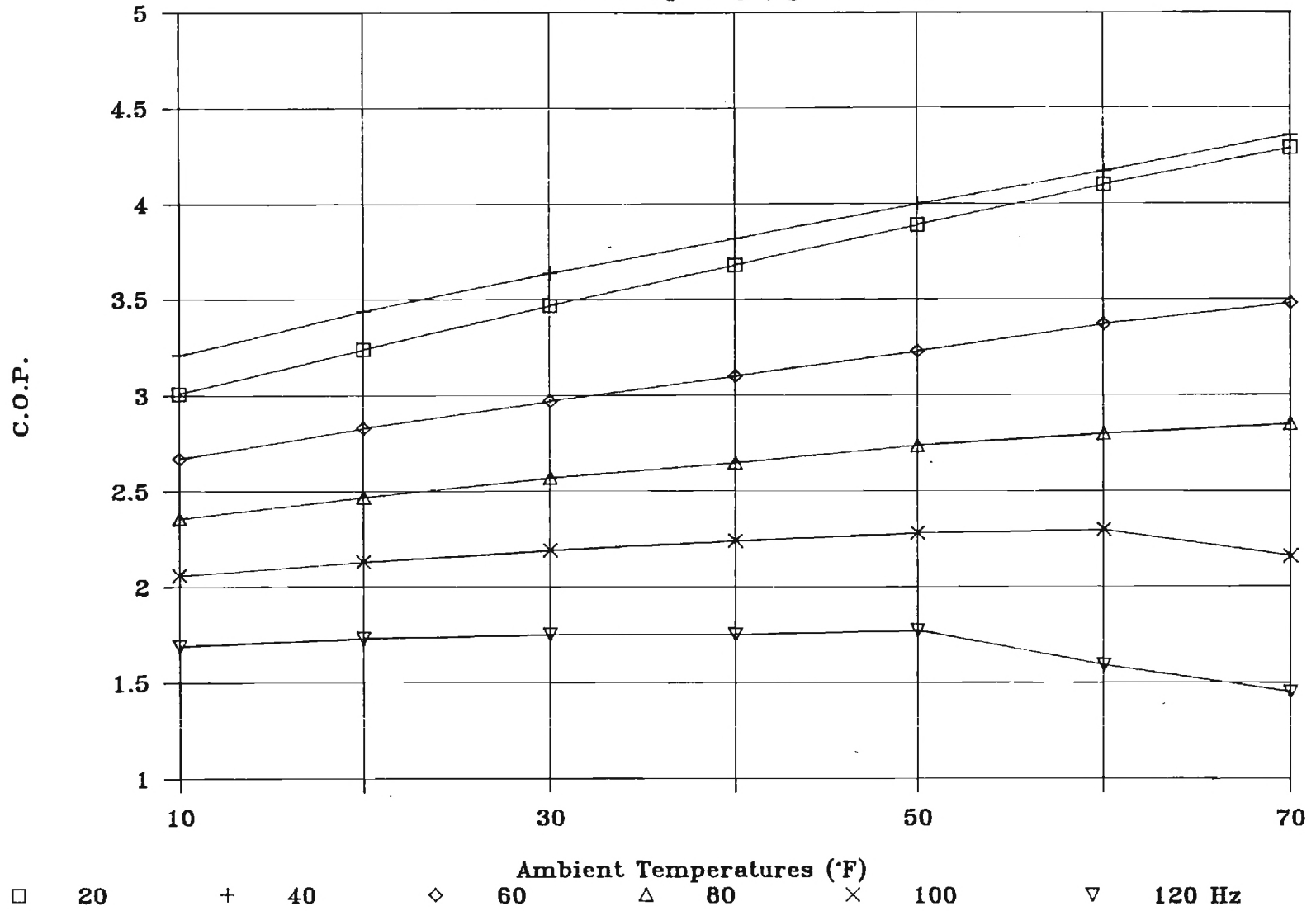


Figure 15
-40-

Variation of Qh

Fixed Fan Frequency (60 Hz)

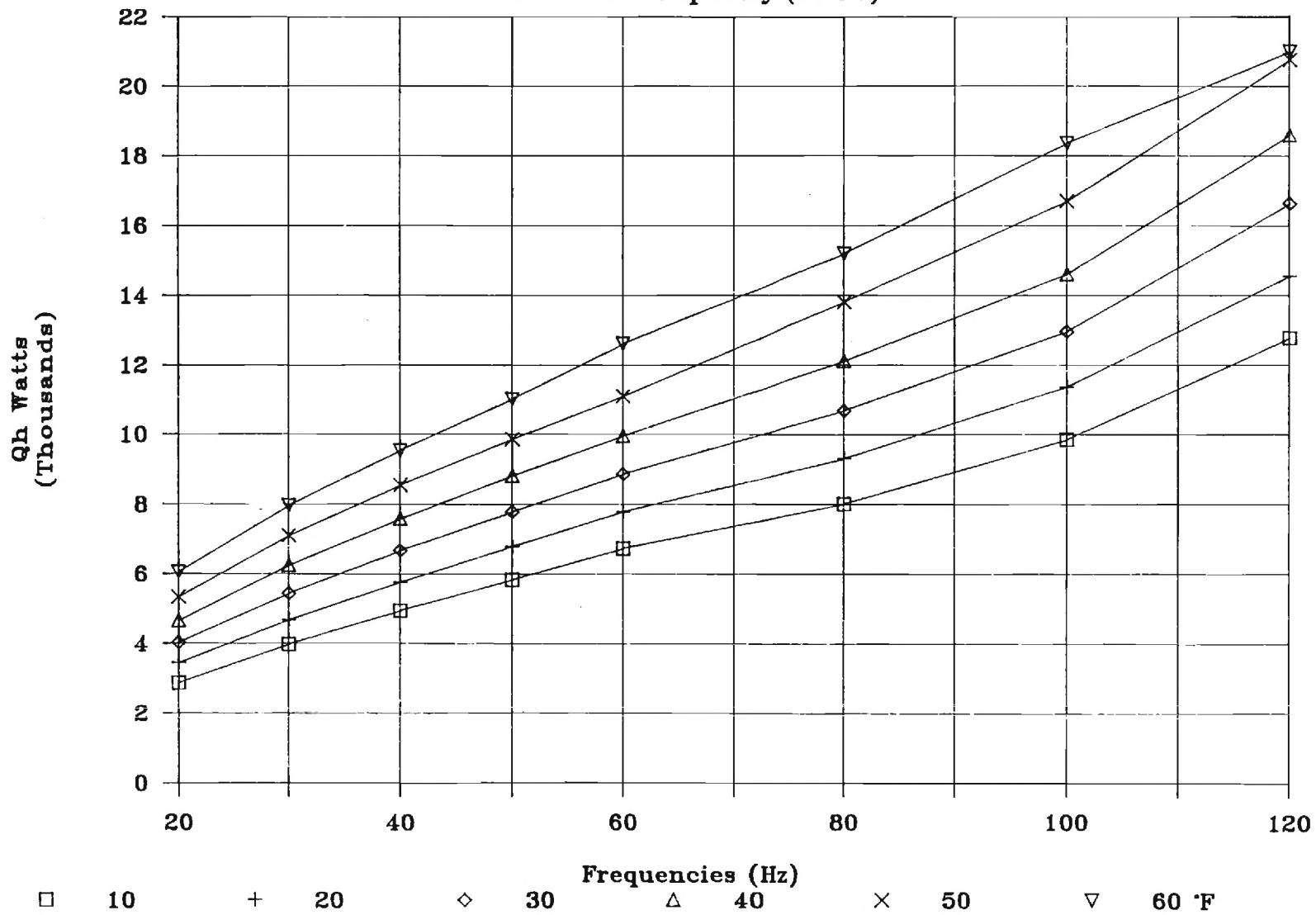


Figure 16

Variation of Qh

Variable Fan Frequency (up to 60 Hz)

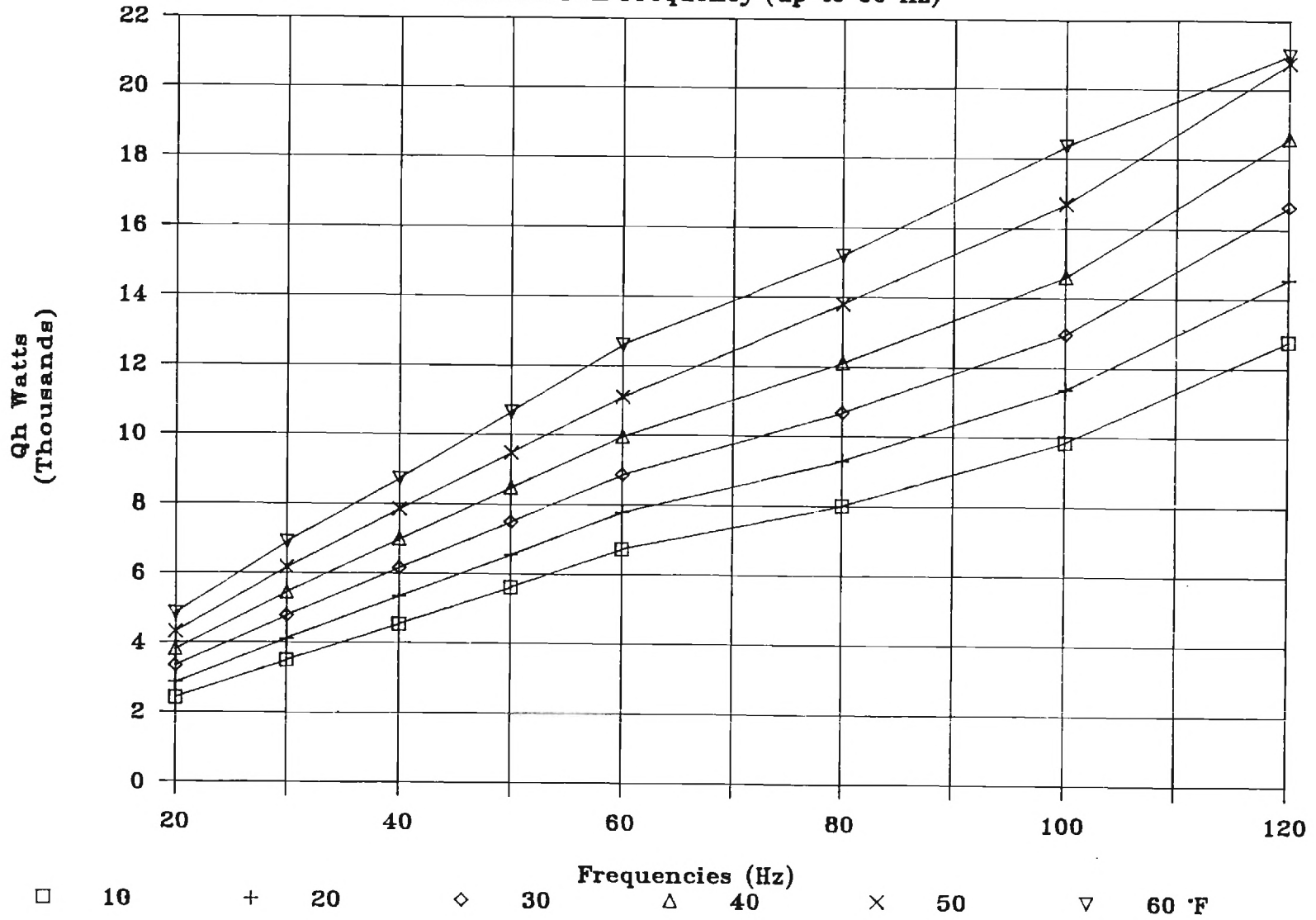


Figure 17

Variation of Qh

Fixed Fan Frequency (60 Hz)

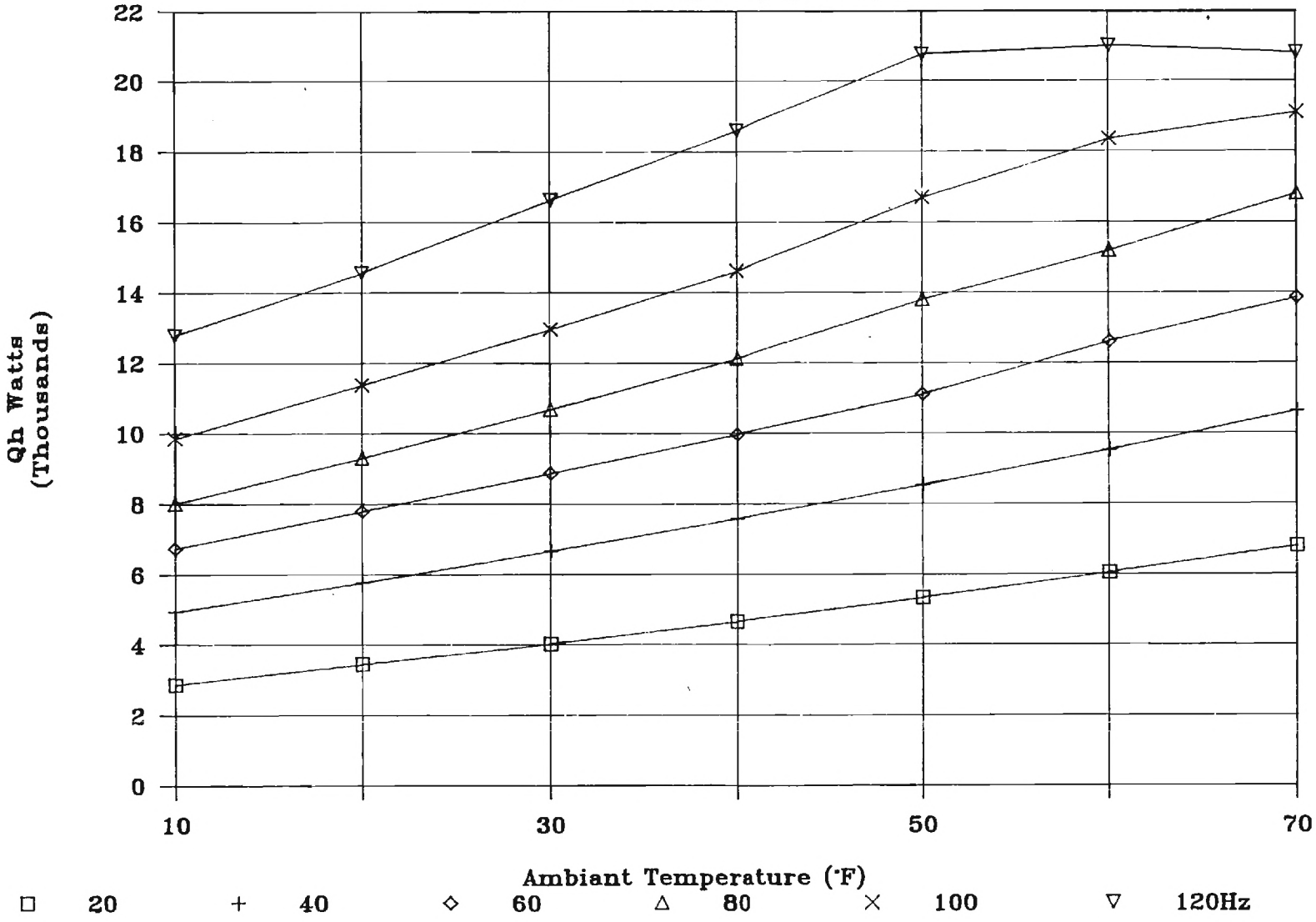


Figure 18

Variation of Qh

Variable Fan Frequency (up to 60 Hz)

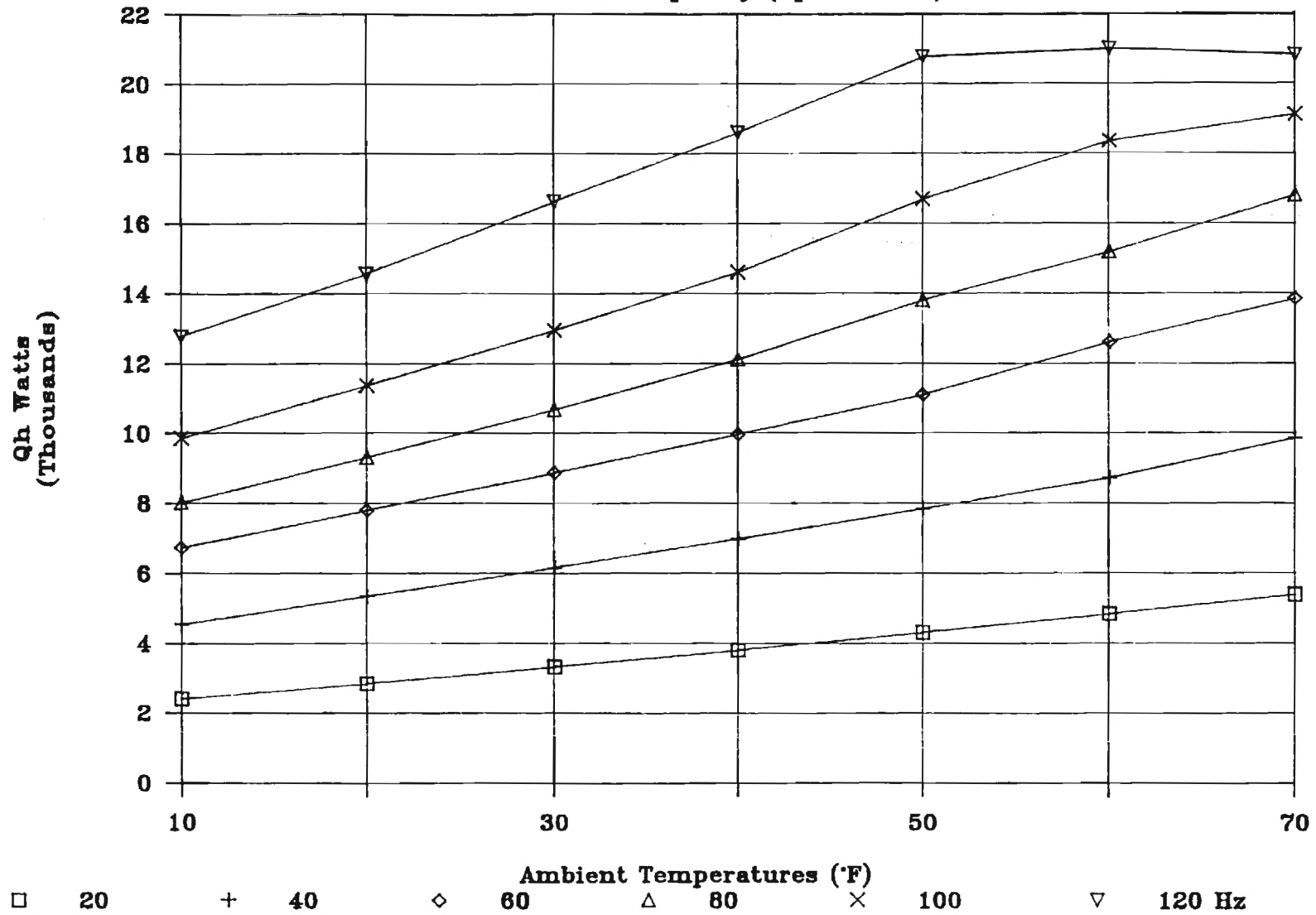


Figure 19

Figure 20

